Journal of Medicinal Chemistry
ACS AuthorChoice
Article
pubs.acs.org/jmc

Establishment of a Structure–Activity Relationship of 1*H*-Imidazo[4,5-*c*]quinoline-Based Kinase Inhibitor NVP-BEZ235 as a Lead for African Sleeping Sickness

João D. Seixas,[†,‡] Sandra A. Luengo-Arratta,[†,‡] Rosario Diaz,[‡] Manuel Saldivia,[‡] Domingo I. Rojas-Barros,[‡] Pilar Manzano,[§] Silvia Gonzalez,[§] Manuela Berlanga,[§] Terry K. Smith,[∥] Miguel Navarro,*[,‡] and Michael P. Pollastri*[,†]

[†]Department of Chemistry and Chemical Biology, Northeastern University, Boston, Massachusetts 02115, United States
[‡]Instituto de Parasitología y Biomedicina "López-Neyra", Granada 18100, Spain
[§]Tres Cantos Medicines Development Campus, DDW and CIB, GlaxoSmithKline, 28760 Tres Cantos, Spain
[∥]Biomedical Sciences Research Complex, University of St Andrews, North Haugh, St Andrews, Fife, KY16 9ST, United Kingdom

Supporting Information

ABSTRACT: Compound NVP-BEZ235 (**1**) is a potent inhibitor of human phospoinositide-3-kinases and mammalian target of rapamycin (mTOR) that also showed high inhibitory potency against *Trypanosoma brucei* cultures. With an eye toward using **1** as a starting point for anti-trypanosomal drug discovery, we report efforts to reduce host cell toxicity, to improve the physicochemical properties, and to improve the selectivity profile over human kinases. In this work, we have developed structure–activity relationships for analogues of **1** and have prepared analogues of **1** with improved solubility properties and good predicted central nervous system exposure. In this way, we have identified **4e**, **9**, **16e**, and **16g** as the most promising leads to date. We also report cell phenotype and phospholipidomic studies that suggest that these compounds exert their anti-trypanosomal effects, at least in part, by inhibition of lipid kinases.

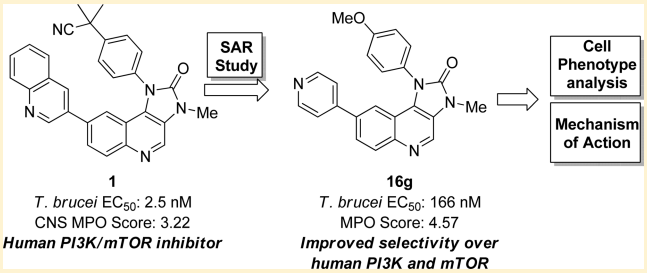

INTRODUCTION

Human African trypanosomiasis (HAT), also known as sleeping sickness, is caused by an infection with a subspecies of the eukaryotic protozoan parasite, *Trypanosoma brucei*. *Trypanosoma brucei gambiense* occurs in Western and Central Africa and is responsible for over 90% of all reported cases of infection, whereas *Trypanosoma brucei rhodesiense* is found in Eastern and Southern Africa. Both subspecies are transmitted by the bite of infected tsetse flies, and it is estimated that about 60 million people are at risk in sub-Saharan Africa, with at least 10 000 cases occurring annually.[1] Established therapies were introduced in the mid-to-late 20th century and have severe safety and efficacy limitations, and drug resistance is emerging against some treatments.[2]

Thus, there is an urgent need to develop new safe, effective, and affordable therapeutics that can be orally administered and are stable under tropical conditions.[3] However, financial incentives for drug discovery against HAT are quite limited because of the economically disadvantaged regions where this disease is endemic. As a strategy to overcome this disincentive for drug discovery, we have hypothesized that medicinal chemistry knowledge against classes of human drug targets could be repurposed to facilitate rapid and cost-effective drug discovery against parasite drug targets. In this "target repurposing" approach, existing drugs and drug-like compounds serve as early hits or leads from which to optimize parasite-specific therapeutics.[4]

Kinase inhibitors represent one promising class of compounds in both humans and parasites. As a pivotal class of enzymes central to cellular signaling, kinases have been identified as key targets for inflammation,[5,6] cancer,[7] and a wide range of other therapeutic indications. Indeed, kinases are estimated to represent 22% of the druggable human genome.[8] The genome of *T. brucei* encodes 176 kinases, and the kinome of the related parasites *Trypanosoma cruzi* and *Leishmania* spp. consists of highly orthologous enzymes,[9,10] some of which are beginning to emerge as druggable targets of potential intervention for such parasitic infections.[11−15]

We recently reported that NVP-BEZ235 (**1**, Figure 1A), currently a phase III clinical candidate for cancer, showed a subnanomolar growth inhibitory phenotype in *T. brucei* and good-to-modest activities against cultures of *T. cruzi* and *Leishmania major*.[12] Recognizing, of course, that **1** is a potent human kinase inhibitor, we started to study the structure–activity relationships (SAR) of this class of compounds in an

Received: March 7, 2014
Published: May 7, 2014

   dx.doi.org/10.1021/jm500361r | *J. Med. Chem.* 2014, 57, 4834−4848

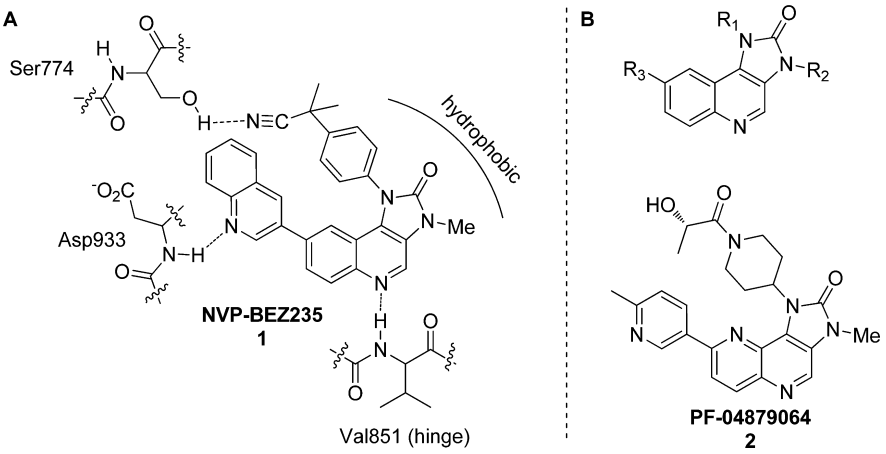

Figure 1. (A) Compound **1** and its proposed interactions with human PI3K-γ.[16] (B) General regions of the compound's core and the structure of **2**, a recently disclosed mTOR/PI3K inhibitor.[17]

Scheme 1[a]

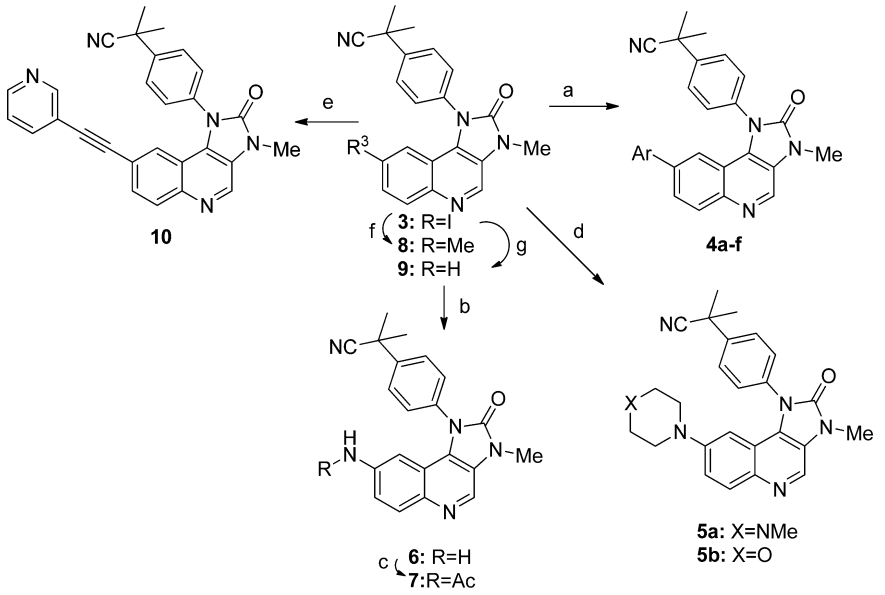

[a]Reagents and conditions: (a) $ArB(OH)_2$, $Pd(PPh_3)_4$, K_2CO_3, glyme/EtOH/H_2O; (b) NH_3/H_2O, CuO, N^1,N^2-diisopropyloxalohydrazide, K_3PO_4, TBAB, H_2O; (c) AcCl, K_2CO_3, DCM; (d) morpholine or *N*-methylpiperazine, butyl di-1-adamantylphosphine, $Pd(OAc)_2$, toluene; (e) 3-acetyleneylpyridine, $Pd(PhCN)_2Cl_2$, *t*-Bu_3P, CuI, dioxane/NMP; (f) MeZnCl, $Pd(PPh_3)_4$, THF; (g) $Pd(PPh_3)_4$, K_2CO_3, glyme/EtOH/H_2O.

attempt to reduce the inherent host cellular toxicity and to allow assessment and subsequent improvement of the selectivity profile over human kinases. Furthermore, the physicochemical properties of **1** do not lend it to CNS exposure (a requirement for HAT therapeutics), as suggested by GSK internal models of CNS penetration and by other predictive models recently disclosed, such as the central nervous system multiparameter optimization (CNS MPO) score.[18]

RESULTS AND DISCUSSION

In order to establish the SAR of this chemotype, we looked toward the docking studies of **1** that were previously reported using a homology model of the human kinase domain of PI3Kγ, showing that the binding of the inhibitor to the hinge region of the kinase is made mainly through three H-bond interactions (Figure 1A).[16] We anticipated that such interactions would also be important for the parasitic kinase(s) by which **1** effected its potent growth inhibition. We therefore divided the structure of **1** into three regions (R^1, R^2, and R^3), as shown in Figure 1B, for systematic modulation.

The docking studies mentioned above showed that the nitrogen atom of the quinoline substituent in the R^3 position could play an important role in binding to Asp933. Very recently, a new mTOR/PI3K dual inhibitor, PF-04979064 (**2**, Figure 1B), was disclosed by Pfizer that contains a 3-pyridine in the same position as the 3-quinolinyl, reinforcing the importance of this substituent for activity against the human targets.[17] To evaluate the importance of this region of the molecule to confer activity against the parasite, we replaced the quinoline with a variety of aromatic and nonaromatic substituents.

Preparation of compounds **4**–**10** was accomplished via various cross-coupling reactions using common intermediate **3** (Scheme 1); Suzuki conditions were employed in the preparation of compounds **4**, direct amination using a

dx.doi.org/10.1021/jm500361r | J. Med. Chem. 2014, 57, 4834−4848

Table 1. Screening Data for R^3 Variants of 1

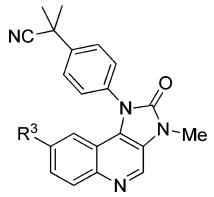

Compound	R^3	T brucei EC_{50} (μM)[b]	HepG2 TC_{50} (μM)[b]	Selectivity[e]	MPO Score
1	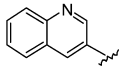	0.0025	nd[a]		3.2
4a	4-pyridyl	0.136	3.43	25	3.9
4b	3-pyridyl	0.016	0.575	36	3.9
4c	Ph	0.159	1.82[d]	11	3.6
4d[f]	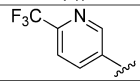	0.053	>25	>470	3.1
4e	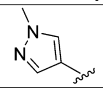	0.051	0.631	12	4.1
4f[f]	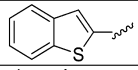	0.054	>25	>460	3.2
5a	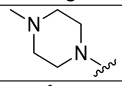	9.772[c]	>50	>5	4.1
5b	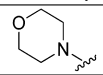	2.042	>50	>24	4.2
6		10.59	>50	>4	5.1
7	-NHAc	9.02	>50	>5	4.6
8	-Me	2.018	>20	>10	4.2
9	-H	0.624	>50	>80	4.6
10[f]	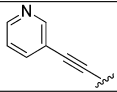	0.008	0.14[d]	17.5	3.4

[a]Data not obtained due to low solubility. [b]EC_{50} values are an average of two replicates, with SD less than 0.1 log unit. [c]SD was less than 0.2 log units. [d]SD was over 1 log unit. [e]Selectivity = TC_{50}/EC_{50}. [f]Stock concentration: 2.5 mM.

Scheme 2. [a,b]

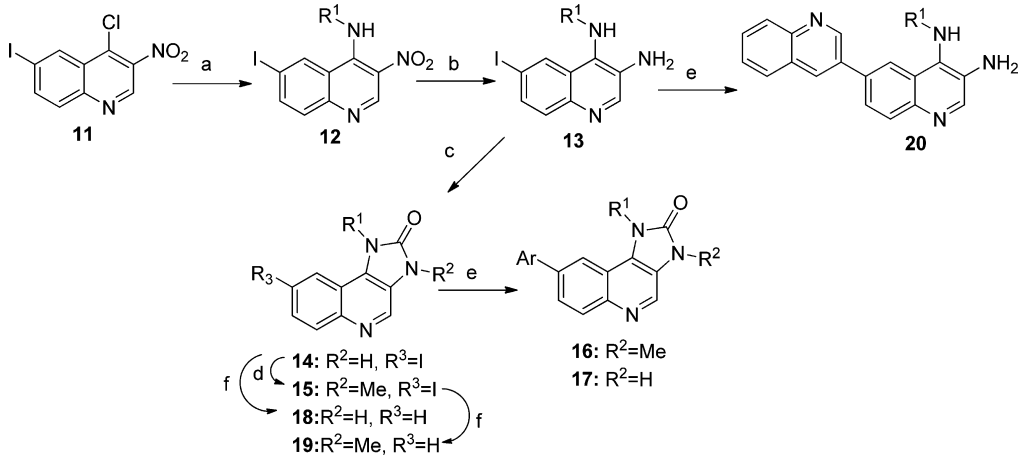

[a]Reagents and conditions: (a) R^1NH_2, AcOH; (b) Fe, NH_4Cl, $EtOH/H_2O$; (c) Cl_3OCOCl, Et_3N, DCM; (d) MeI, 0.15 M NaOH(aq), DCM, TBAB; (e) $ArB(OH)_2$, $Pd(PPh_3)_4$, K_2CO_3, 1,2-DME, EtOH, H_2O; (f) $Pd(PPh_3)_4$, K_2CO_3, 1,2-DME, EtOH, H_2O. [b]See the tables for the R^1 substituents.

Buchwald–Hartwig reaction for compounds **5**, or copper-catalyzed conditions in aqueous ammonia for compound **6**. Compound **10** was prepared utilizing Sonogashira coupling conditions. Palladium-mediated dehalogenation of **3** provided **9**. Compound **8** was easily obtained utilizing Negishi coupling conditions with chloro(methyl)zinc and palladium catalyst. Biological assessments of these compounds are summarized in Table 1 and are discussed below.

dx.doi.org/10.1021/jm500361r | J. Med. Chem. 2014, 57, 4834–4848

Table 2. Biological Data for R^1 and R^3 Variations

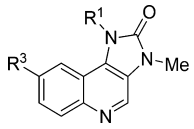

Compound	R^1	T brucei EC_{50} (μM)[b]	HepG2 TC_{50} (μM)[d]	Selectivity[e]	MPO Score
R^3 = 3-quinolinyl					
1	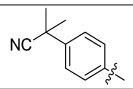	0.0025	nd[a]		3.2
16a[f]	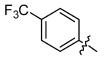	0.103	>25	>240	3.2
16b	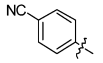	0.091	>50	>540	3.5
16c[f]	Ph	0.024	>25	>1000	3.7
R^3= 4-pyridyl					
4a	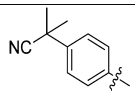	0.136	3.43	25	3.9
16d	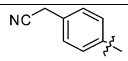	0.088	>50	>560	4.8
16e		0.202	4.78	24	4.1
16f[g]	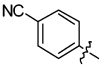	0.072[c]	nd		4.8
16g	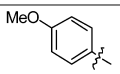	0.166	11.2	67	4.6
16h[f]	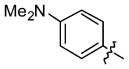	0.082	2.34	28	4.2
16i[h]	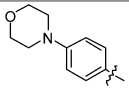	0.316	>7.6	>24	4.4
16j	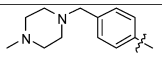	3.35	>7.6	>2	3.9
16k[i]	Me	3.273	>20	>6	6

[a]Data were not obtained due to low solubility. [b]EC_{50} average was obtained from two replicates, with SD lower than 0.1 log units. [c]SD lower than 0.2 log. [d]TC_{50} average was obtained from two replicates, with SD lower than 0.5 log units. [e]Selectivity = TC_{50}/EC_{50}. [f]Stock concentration: 2.5 mM. [g]Stock concentration: 0.35 mM. [h]Stock concentration: 0.75 mM. [i]Stock concentration: 2 mM.

Synthesis of analogues with variations of both R^1 and R^3 was achieved starting from **11**, which was prepared via a three-step sequence starting from 2-amino-5-iodobenzoic acid with an overall yield of 51% (Scheme 2).[19] Preparation of anilines **12** was accomplished via nucleophilic aromatic substitution with the requisite amine, and nitro group reduction using iron provided intermediates **13**. Cyclization of the imidazolidinone ring was obtained with diphosgene (compounds **14**), and *N*-methylation gave intermediates **15**. Final compounds (**16** and **17**) were synthesized from **14** and **15** using Suzuki cross-couplings in a microwave reactor. We also prepared the ring-opened analogue **20** from **13** using Suzuki conditions. Structure and biological activity of the compounds prepared in Scheme 2 are summarized in Table 2.

Biological Assessments. As shown in Table 1, replacing the quinoline with a 3-pyridine (**4b**), with the nitrogen atom in the same spatial region, decreased potency by 8-fold (EC_{50} = 16 nM) compared to that of **1** and exhibited high HepG2 cytotoxicity (TC_{50} = 575 nM). The same 3-pyridine with an ethyne spacer (**10**) only loses 4-fold activity (EC_{50} = 8 nM), but it displays even worse selectivity. In fact, **10** is a clinical backup molecule for **1** from Novartis,[20] so this host cell activity is not unexpected.

However, introducing a trifluoromethyl group in the para position of the 3-pyridine (**4d**) eliminated HepG2 cytotoxicity (TC_{50} > 25 μM) while maintaining a good activity against the parasite (EC_{50} = 53 nM).

Installation of a 4-pyridine (**4a**) at the R^3 position also rendered a potent molecule (EC_{50} = 136 nM), with 25-fold selectivity over host cells. Overall, the pyridine substituents presented a more favorable profile than an unadorned aromatic phenyl ring (**4c**), which has lower potency and reduced selectivity.

Following the promising profile exhibited by the pyridine-substituted analogues, other heteroaromatic substituents were explored. For example, the five-membered ring methyl-imidazole afforded a highly potent compound, **4e** (EC_{50} = 51 nM), albeit with only a 12-fold selectivity window. However, more bulky benzothiophene **4f** was similarly potent (54 nM), yet with no HepG2 toxicity observed.

dx.doi.org/10.1021/jm500361r | J. Med. Chem. 2014, 57, 4834−4848

Table 3

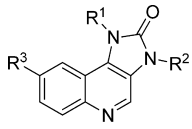

Compound	R1	R2	R3	T brucei EC_{50} (μM)[a]	HepG2 TC_{50} (μM)[b]	Sel[c]	MPO Score
16d	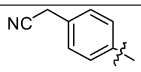	Me		0.088	>50	>560	4.8
17d		H	4-pyridyl	0.199	>50	>250	4.6
16h[f]	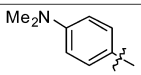	Me		0.082	2.34	29	4.2
17h[g]		H	4-pyridyl	0.042	>50	>1100	4.2
19	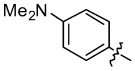	Me		9.33	3.0	0.3	4.9
18		H	H	6.24	19.05	3	4.6
16b	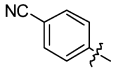	Me	3-quinolinyl	0.091	>50	>540	3.5
17b		H		0.184	>50	>270	3.5
21	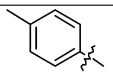	Me	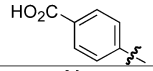	9.89	>50	>5	4.7
22	Ph	Me	Me	1.30	>50	>39	4.5
23	Ph	Me	H	18.5	>50	>3	5.0

[a]EC_{50} average was obtained from two replicates, with SD lower than 0.1 log. [b]TC_{50} average was obtained from two replicates, with SD lower than 0.5 log. [c]Selectivity = TC_{50}/EC_{50}. [f]Stock concentration: 2.5 mM. [g]Stock concentration: 1.25 mM.

Introducing cyclic or linear amines or amides at the R^3 position led to complete loss of activity against *T. brucei* and HepG2. Eliminating R^3 substituents from **1** altogether (**9**) resulted in a ∼300-fold loss of potency, although this compound still remained in submicromolar range (EC_{50} = 624 nM). We observe that an aromatic system (preferably heteroaromatic) is needed in the R^3 region to afford potent anti-trypanosomal activity (cf. **8**). Nevertheless the choice of this group influences HepG2 cytotoxicity and the overall physicochemical profile of the molecule.

In the R^1 position, we first evaluated the importance of the substituents in the para position of the aromatic ring in R^1 with **16a−c** (Table 2). These derivatives exhibited a 10−15-fold decrease in potency when compared to that of **1**. Surprisingly, the most potent compound was the one without a para substituent (**16c**, EC_{50} = 24 nM), and both the nitrile (**16b**) and trifluoromethyl (**16a**) analogues showed similar anti-trypanosomal potency (EC_{50} = 91 and 103 nM, respectively). In addition, these three compounds exhibited an excellent selectivity profile against HepG2. This data shows that when R^3 = 3-quinolinyl the presence of a substituent in the para position of the phenyl ring of the R^1 position is important, but not essential, for anti-trypanosomal activity. Interestingly, when the R^3 group is 4-pyridyl, the presence of a nitrile group (**16d** and **16f**) or amine moiety (**16h**) in the R^1 para position seems to afford improved potency over *p*-methyl or methoxy (**16e** and **16g**). This is perhaps consistent with the predicted binding of **1** to the human p110α orthologue, where the nitrile established hydrogen bonds with Ser774, contributing to a strong binding to the human target.[16] We observe a loss in activity when substituents on both the R^1 and R^3 substituents are eliminated simultaneously (**23**, Table 3).

One of the medicinal chemistry goals of this work was to improve the physicochemical properties of the new compounds. Compound **1** is very lipophilic (cLogP = 5.81, chromLogD = 4.75)[21] and displays very poor solubility (19 μM) (Supporting Information, Table S2).[22] The high number of aromatic rings surely contributes to the establishment of favorable π-stacking interactions, resulting in low solubility. Not unexpectedly, R^3 quinolinyl compounds **16a−c** also presented very low solubility. However, with a 4-pyridyl substituent at R^3, a drastic reduction in cLogP was observed (compare **1** vs **4a** and **4c**), and one of these compounds (**4a**) maintained good antiparasitic activity (EC_{50} = 136 nM, TC_{50} = 3.43 μM).

Using **4a** as reference, increase of potency was achieved by removing the two α-methyl groups (**16d**) or by replacing the $-C(CH_3)_2CN$ group by a dimethyl amine (**16h**). We hypothesize that the improved positioning of a nitrogen lone pair for hydrogen bonding lends **16h** to having improved potency. However, introduction of a methyl (**16e**) slightly decreases potency relative to that of **4a**, and incorporation of a methoxy group (**16g**) has little impact on activity. Addition of a larger, nonaromatic heterocycle or replacement of the R^1 group with methyl reduces or abrogates activity (**16i−k**).

The R^2 substituent on the urea ring adjacent to the quinoline core was also explored in terms of methylation versus nonmethylation of the free NH for compounds **16**/**17b**, **16**/**17d**, **16**/**17h**, and **18**/**19** (Table 3). However, no clear trends were evident. Compound **16h** is also the only example where methylation afforded toxicity in HepG2 (TC_{50} = 2.34 μM). Opening the imidazolone ring the carbonyl group in the "urea-imidazo" ring seems to play an important role. Disruption of the aromatic ring, affording the free amine (**20**), led to a significant loss in potency (EC_{50} = 0.767 μM). From a physicochemical property perspective, we do not observe a trend in solubility and permeability when comparing R^2 = Me versus H.

As mentioned above, we note that **1** does not penetrate the blood−brain barrier (BBB), a crucial requirement for new drugs in order to be effective in the second stage of HAT. In evaluating analogue designs, we employed the multiparameter optimization (MPO) algorithm developed by Pfizer scientists

dx.doi.org/10.1021/jm500361r | J. Med. Chem. 2014, 57, 4834−4848

Table 4. Comparison of Properties of 1 and Prioritized Compounds

	1	4e	9	16e	16g
Potencies					
T. brucei EC_{50} (μM)	0.0025	0.051	0.617	0.200	0.166
HepG2 TC_{50} (μM)	nd[b]	0.631	>50	4.786	11.220
LE[c]	0.32	0.30	0.33	0.33	0.32
mTOR IC_{50} (μM)	0.005	1.175	1.622	0.468	0.380
PI3Kα IC_{50} (μM)	0.020	0.398	3.981[e]	0.631	0.501
PI3Kβ IC_{50} (μM)	0.316	7.943	>30	31.623	7.943
PI3Kγ IC_{50} (μM)	0.100	0.126	1.995	0.251	0.316
PI3Kδ IC_{50} (μM)	0.013	0.794	15.849	2.512	2.512
Properties					
MPO score	3.22	4.08	4.56	4.07	4.57
MW	469.6	422.5	342.4	366.4	382.4
cLogP	5.81	5.3	5.62	5.86	5.1
chromLogD[d,21]	4.75 (6.44)	(5.3)	(4.69)	3.5 (4.95)	3.03 (5.32)
TPSA	76.52	81.43	63.61	52.71	61.94
HBD	0	0	0	0	0
solubility (μM)[22]	19	nd[a]	nd[a]	17	22
permeability	nd[a]	nd[a]	570	470	860

[a]nd = data not obtained. [b]Not obtained due to low solubility. [c]LE = $-\mathrm{Log}(\mathrm{pEC}_{50}) \times 1.37$/number of heavy atoms. [d]LogD values in parentheses are calculated values. [e]One replicate experiment showed an IC_{50} >30 μM.

for CNS-active drugs.[18,23] This aforementioned publication showed a correlation between six fundamental physicochemical properties (cLogP, cLogD, MW, TPSA, hydrogen-bond donors, and the pK_a of the most basic center) and their impact on CNS-acting agents as well as other critical ADME, toxicity, and binding efficiencies. By summing scores for each of these six properties, one can ascertain the likelihood that a given compound should penetrate the CNS. Importantly, a subsequent report successfully applied this approach prospectively for design of CNS-penetrant PI3K-α inhibitors.[24]

As a point of reference, the CNS MPO score of **1** is 3.22, which is lower than the desirable range of CNS-active molecules (≥4). From the new analogues synthesized and tested here, only four shown in Tables 1−3 scored equal to or worse than **1**, and these were primarily due to unfavorable LogP, LogD, and molecular weight values. The MPO score of our most potent analogue (**4b**) improved to a score of 3.9, which is a direct effect of MW and cLogP decrease compared to those of **1**. However, although **16d** is slightly less potent than **4b**, we observe significant improvement in cellular selectivity and predicted CNS activity (MPO score = 4.8).

Biochemical Kinase Selectivity. On the basis of the cellular potency and selectivity profiles, we prioritized 14 compounds, plus **1**, to be tested against PI3K-α, -β, -γ, and -δ as well as mTOR, and this data is shown in the Supporting Information (Table S1). We note that although seven of these compounds retain nanomolar levels of mTOR activity, in most cases we do observe decreases in potency against the mammalian kinases tested.

Next, on the basis of an evaluation of anti-trypanosomal activity, selectivity, MPO score, and the biochemical selectivity assays, we selected four compounds (plus compound **1**) to initiate mechanism of action studies. These four prioritized compounds are shown in Table 4.

Phospholipidomics Analysis. We originally selected **1** to investigate its potential as an trypanocidal agent on the basis of its activity as a PI3K/mTOR inhibitor in mammalian cells and the fact that PI3K activity is essential for the bloodstream form of the *T. brucei* parasite.[25] In the interest of elucidating the potential mechanism of action against *T. brucei* cells, we performed a lipidomic analysis to discern if PI kinases are likely targets of these analogues. Lipid extracts of cells grown in the presence of the best compounds at sublethal doses (200 nM) for 12 h were analyzed by ES-MS. Survey scans in positive and negative ion mode between 600 and 1000 *m/z* showed a wide range of expected phospholipid species (Supporting Information Figures S1 and S2, respectively). There were no significant differences in the phosphatidylcholine (PC) and sphingomylein (SM) species between the control and cells grown in the presence of the other compounds (Figure S1). Additionally, only minor differences were observed in the negative ion mode survey scans between the control and the treated cells (Figure S2). However, variations were observed in the relative ratios of the PI species 862 *m/z* (18:0/18:2), 886 *m/z* (18:0/20:4), and 912 *m/z* (18:0/22:5), as well as relative to 826 *m/z* PG (18:0/22:4). This could be a reflection in changes in either the formation of PI (hence, PG increases as PI decreases) because they have a common lipid donor (cytidine-diphosphate-diacylglycerol) or variation in the usage of PI (i.e., for PIP formation). Alternatively, as is often the case, changes in the lipid profile could be a reflection in the cells succumbing to (or adapting to) a defect in a major cellular process, such as endo- or exocytosis or cell cycle arrest.

Because these compounds are thought to target PI3K, negative ion mode scans between 950 and 1300 *m/z* were conducted to focus upon singly and multiply phosphorylated PIs. As seen in Figure 2A for the control cells, PIP species are observed at ∼992 *m/z* and ∼1040 *m/z*, corresponding to 40:5-8 and 44:7-9, respectively, as well as PIP_3 (44:9-12) species at ∼1215 *m/z*.

Compounds **1** and **16g** (Figure 2B,C) show almost complete absence of all phosphorylated PIs, clearly indicating that these compounds are targeting PI kinases (e.g., PI3K). Compounds **4e** and **16e** (Figure 2C,E) also show significant (albeit incomplete) reduction in PIP levels, although this reduction is significant compared to that in the control cells (Figure 2A), indicating that they are affecting metabolism of PIPs, most likely phosphorylation of PI.

dx.doi.org/10.1021/jm500361r | J. Med. Chem. 2014, 57, 4834−4848

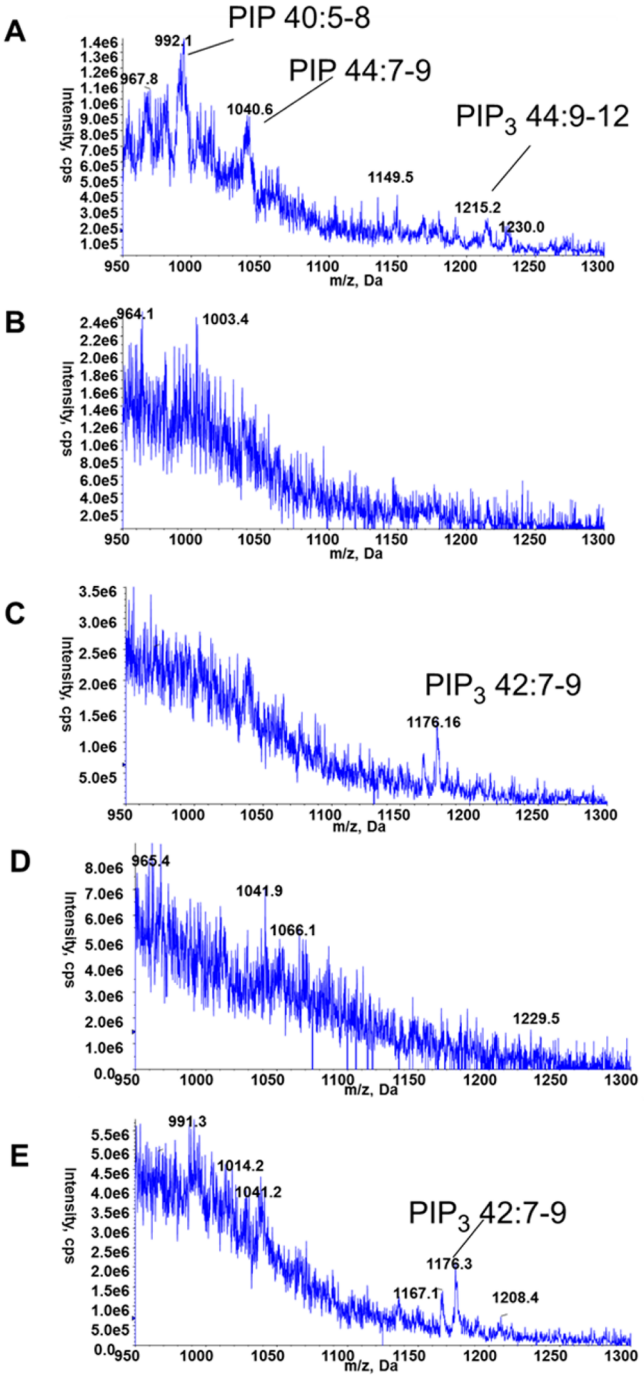

Figure 2. Negative ion mode survey scans from 950 to 1300 *m/z*: (A) DMSO (control), (B) **1**, (C) **4e**, (D) **16g**, and (E) **16e**.

Cell Phenotype Analysis. BEZ235 is known to inhibit human PI3K/mTOR; thus, we used the human kinase domain of PI3K-γ (including Ser774, Val855, and Asp933, mentioned above) to search in the *T. brucei* genome geneDB for homologous enzymes. Two high-homology PI3Ks were identified: the previously characterized TbPI3KIII (Tb927.8.6210), which is orthologous to the yeast Vps34, and an uncharacterized, potentially pseudo TbPIK (Tb927.11.15330). In addition, three of the four TORs described in trypanosomes, TbTOR1, TbTOR2, and TbTOR3, were also identified. In the sequences of these five proteins, similar positions for the important residues, Ser774, Val855, and Asp933, were observed. To resolve the possible target(s) of compound **1**, we compared the phenotype of cells treated with **1** with the previously described phenotypes caused by RNAi of these various kinases. TbPI3KIII depletion in *T. brucei* induced a phenotype characteristic of a defective endocytosis,[25] similar to the phenotype observed in cells treated with **1**. Furthermore, ES-MS analyses show complete absence of PIPs, suggesting that **1** is indeed targeting one or more of the PI/PIP kinases, including TbPI3KIII (Figure 2).

Highly efficient and rapid endocytosis is one of the most important cellular processes for this infective parasite to survive and multiply within the bloodstream of the host, and the activity of TbPI3KIII is essential for this process.[25] To gain insight on the possible target(s) of our compounds, we carried out transferrin uptake experiments to measure receptor-mediated endocytosis after drug treatment. The analogues of **1** showed varied trypanocidal potency, so we decided to use concentrations twice that of the EC_{50} of each of the four compounds in Table 4 over a short treatment period (18 h). These transferrin uptake assays showed that **1** inhibited endocytosis dramatically, as did compounds **16e** and **16g** (Figure 3). In addition, the fact that PIP3 levels were

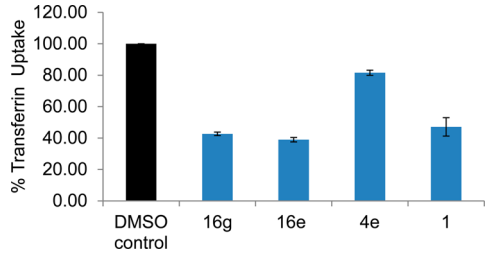

Figure 3. Transferrin uptake of the bloodstream form of *T. brucei* treated with BEZ235 derivative compounds. The histogram shows the percentage of transferrin uptake relative to that in untreated cells (DMSO) as a control. Mean ± SD of three independent measurements is shown.

dramatically reduced after treatment with compounds **1** and **16g** further supports the hypothesis they are affecting PIK activity, including TbPI3KIII (Figure 2). Compound **16e** induced a phenotype defective in endocytosis (Figure 3); however, the PIP_3 molecular species identified (42:7-9) was not the same PIP_3 molecular species identified in WT cells (44:9-12). These data suggest that **16e** reduces PIP_3 44:9-12 formation by inhibiting similar target(s) to that of compounds **1** and **16g**, but it may have an additional mode of action because it causes PIP_3 42:7-9 to be observed, which may be present in a different subcellular compartment or organelle.

Conversely, compound **4e** showed a different phenotype, as it did not significantly reduce transferrin endocytosis compared to that of the control (Figure 3). In addition, compound **4e** affected cell cycle progression by reducing the proportion of cells in G1 and increasing multinucleated cells, whereas compounds **1**, **16g**, and **16e** did not significantly alter cell cycle progression over this short treatment time (18 h) (Supporting Information Figure S3).

Collectively, these data suggest that compound **4e** has a different mode of action than **1**, **16e**, and **16g** because endocytosis was not affected, although the induction of changes in the PIP3 species (Figure 2) suggests PIP metabolism was affected.

dx.doi.org/10.1021/jm500361r | J. Med. Chem. 2014, 57, 4834−4848

Previously published functional analysis showed that TbTOR2 depletion affected endocytosis and cytokinesis,[26] whereas rapamycin (a specific inhibitor of TbTOR2 in trypanosomes) treated cells induce different changes in the lipid profile than those from compound **1** (data not shown). The RNAi of additional TbTOR1 and TOR3 protein kinases[26,27] does not resemble the defect in endocytosis observed by the treatment with **1**, suggesting that the TbTOR family of PIKK is not the main target of **1**.

These studies cannot determine unequivocally which member of the trypanosome PI3K family may be the actual molecular target; however, our data strongly suggests that TbPI3KIII is the main target of BEZ235 as well as of derivative compounds **16e** and **16g**. Regardless, it is possible that additional molecular target(s) in the parasite may be affected

In summary, we have developed initial SAR for analogues of **1** as anti-trypanosomal agents. We have identified regions of the molecule that allow improvement of selectivity over selected kinases and HepG2 cells, and we have measured and computed physicochemical properties that place analogues in a CNS-penetrant region of properties space, as predicted by the CNS MPO scoring regime. With this in mind, we highlight the compounds in Table 4 as our most promising leads in this series, as they possess significant overall improvements over **1**. We now have preliminary lipidomics and cell phenotype data to suggest primary targets of action within the lipid kinase pathways, and additional target identification work is continuing using orthogonal methods. Work is also ongoing to establish whether the predicted favorable properties hold true in pharmacokinetic and animal efficacy studies, which will be reported in due course.

EXPERIMENTAL SECTION

Chemistry. Starting materials were obtained from commercial suppliers and used without further purification unless otherwise stated. Flash column chromatography was carried out using prepacked Isolute Flash or Merck Si60 (15−40 μm) silica gel columns as the stationary phase and analytical grade solvents as the eluent unless otherwise stated. Proton magnetic resonance (^{1}H NMR) spectra were recorded at 400 MHz on a Bruker AMX400 spectrometer and are reported as follows: chemical shifts δ (ppm) (multiplicity, coupling constant in J (Hz), number of protons). Multiplicities are labeled s, singlet; d, doublet; t, triplet; m, multiplet; br, broad; or a combination of these. Total ion current traces were obtained for electrospray positive and negative ionization (ES+/ES−) on a Waters SQ detector. Analytical chromatographic conditions used for the LC/MS analysis were as follows. The column was an Acquity UPLC BEH C18 1.7 μm, 3 × 50 mm. Solvent A was an aqueous solvent consisting of 25 mM ammonium acetate. Solvent B was 90% acetonitrile + 10% water (pH 6.6). Additional chromatographic parameters were as follows: flow rate, 0.8 mL/min; injection volume, 2 μL; column temperature, 40 °C; and UV wavelength range, 200−330 nm. The purity of all tested compounds was ≥95% using the analytical method described above unless otherwise stated. Compounds **10** and **11**[20] were prepared as previously described, and their characterization is included in the Supporting Information.

General Procedure A: Aryl Halide Displacement. To a suspension of 4-chloro-6-iodo-3-nitroquinoline (**11**) (8 g, 24 mmol) in AcOH (100 mL) was added a solution of amine (1.1 equiv) in 70 mL of AcOH. The suspension was stirred for 3 h at rt under N_2 and quenched with H_2O (150 mL). The resulting yellow precipitate was recovered by filtration, dissolved in CH_2Cl_2, washed with a saturated aqueous solution of $NaHCO_3$ (100 mL) and then H_2O (100 mL), dried over $MgSO_4$, filtered, and concentrated.

General Procedure B: Reduction of Nitroarenes. A suspension of nitroarene **12** (2.6 mmol) in ethanol (37 mL) was heated at reflux. To this mixture was added iron (10 equiv) followed by a solution of NH_4Cl (1.42 g, 26 mmol) in H_2O (11 mL). The resulting suspension was heated at reflux for 2 h. The hot mixture was then filtered through a Celite pad, and the filtrate was evaporated under vacuum. The residue was dissolved in EtOAc (30 mL) and washed with H_2O (30 mL), and the aqueous phase was further extracted with ethyl acetate (2 × 20 mL). The organic extracts were combined, dried over $MgSO_4$, filtered, and evaporated under vacuum.

General Procedure C: Formation of the C ring. A solution of diamine **13** (10.5 mmol) and triethylamine (1.2 equiv) in CH_2Cl_2 (175 mL) was added dropwise at 0 °C to a solution of trichloromethyl chloroformate (1.1 equiv) in CH_2Cl_2 (50 mL), and the resultant solution was stirred for 2 h while being allowed to warm slowly to rt. The reaction was quenched with a saturated aqueous solution of $NaHCO_3$ (150 mL) and stirred for 2 h. Phases were separated, and the aqueous layer was further extracted with CH_2Cl_2 (2 × 60 mL). Organic phases were combined, dried over $MgSO_4$, filtered, and concentrated

General Procedure D: N^1 Methylation. An aqueous solution of NaOH (88 mL, 0.15 M) was added to a mixture of intermediate **14** (8.8 mmol), methyl iodide (1.5 equiv), and tetrabutylammonium bromide (0.1 equiv) in CH_2Cl_2 (180 mL). The resultant mixture was stirred for 24 h at rt in a sealed tube. The reaction was quenched with H_2O (100 mL), phases were separated, and the aqueous layer was further extracted with CH_2Cl_2 (3 × 180 mL). Volatiles were combined and evaporated under reduced pressure.

General Procedure E: Suzuki Coupling. A microwave vessel was loaded with aryl iodide **3** (0.149 mmol), K_2CO_3 (1.5 equiv), $Pd(PPh_3)_4$ 5 mol %), and boronate (1.1 equiv) in 1,2-dimethoxyethane (2 mL), EtOH (1 mL), and H_2O (0.5 mL). The vessel was evacuated, backfilled with nitrogen, and sealed. The mixture was heated in a microwave reactor at 175 °C for 15 min (including the ramp time). After cooling, the solids were removed by filtration, H_2O (10 mL) and CH_2Cl_2 (10 mL) were added, phases were separated, and the aqueous layer was further extracted with CH_2Cl_2 (10 mL). Volatiles were combined and evaporated under reduced pressure. Purification was carried out by flash column chromatography over silica gel.

General Procedure F: Buchwald Coupling. A sealed vial was charged with intermediate **3** (0.256 mmol), morpholine (1.2 equiv), butyl(ditricyclo[3.3.1.1~3,7~]dec-1-yl)phosphane (0.1 equiv), sodium *tert*-butoxide (1.2 equiv), $Pd(OAc)_2$ (5 mol %), and toluene (2.3 mL). The resultant mixture was purged with argon for 5 min and then heated at 115 °C for 3 days. The reaction mixture was quenched with H_2O (3 mL) and extracted with CH_2Cl_2 (2 × 10 mL). The organics were combined, dried over $MgSO_4$, filtered, and concentrated under vacuum. Purification was carried out by flash column chromatography over silica gel.

General Procedure G: Negishi Coupling. A microwave vessel was loaded with aryl iodide **3** (80 mg, 171 μmol), methylzinc chloride solution 2 M in THF (4 equiv), and palladium *tetrakis*(triphenylphosphine) (0.1 equiv) in THF (4 mL). The vessel was evacuated, backfilled with nitrogen, and sealed. The mixture was heated in a microwave reactor at 75 °C for 1 h (including the ramp time). After cooling, the solids were removed by filtration. Saturated solutions of ammonium chloride (5 mL) and EtOAc (10 mL) were added, phases were separated, and the aqueous layer was further extracted with EtOAc (10 mL). Volatiles were combined and evaporated under reduced pressure. Purification was carried out by washing the resultant solid with MeOH.

2-(4-(8-Iodo-3-methyl-2-oxo-2,3-dihydro-1*H*-imidazo[4,5-*c*]-quinolin-1-yl)phenyl)-2-methylpropanenitrile (3). Prepared using General Procedure D from **14** to give **3** as a yellow solid (yield: 81%). ^{1}H NMR (400 MHz, DMSO-d_6) δ ppm: 9.01 (s, 1H), 7.85 (d, J = 8.5 Hz, 2H), 7.76 (m, 2H), 7.68 (d, J = 8.5 Hz, 2H), 7.14 (s, 1H), 3.58 (s, 3H), 1.81 (s, 6H). LCMS found, 469 $[M + H]^+$.

2-Methyl-2-(4-(3-methyl-2-oxo-8-(pyridin-3-yl)-2,3-dihydro-1*H*-imidazo[4,5-*c*]quinolin-1-yl)phenyl)propanenitrile (4b). Prepared from 3-pyridinyl boronic acid using General Procedure E. Purification was carried out by flash column chromatography over

dx.doi.org/10.1021/jm500361r | J. Med. Chem. 2014, 57, 4834−4848

silica gel (eluent: CH_2Cl_2/MeOH 100:0 to 95:5) to give **4b** as an off-white solid (yield: 40%). ^{1}H NMR (400 MHz, DMSO-d_6) δ ppm: 9.01 (s, 1H), 8.54 (m, 2H), 8.15 (d, J = 8.8 Hz, 1H), 7.97 (dd, J = 8.8, 2.0 Hz, 1H), 7.88 (m, 2H), 7.75 (m, 3H), 7.41 (m, 1H), 7.12 (d, J = 1.8 Hz,1H), 3.62 (s, 3H), 1.83 (s, 6H). LCMS found, 420 $[M + H]^+$.

2-Methyl-2-(4-(3-methyl-2-oxo-8-phenyl-2,3-dihydro-1*H*-imidazo[4,5-*c*]quinolin-1-yl)phenyl)propanenitrile (4c). Prepared from phenylboronic acid using General Procedure E. Purification was carried out by flash column chromatography over silica gel (eluent: CH_2Cl_2/MeOH 100:0 to 95:5) to give **4c** as an off-white solid (yield: 51%). ^{1}H NMR (400 MHz, $CDCl_3$) δ ppm: 8.81 (s, 1H), 8.19 (d, J = 9.0 Hz, 1H), 7.86 (dd, J = 9.0, 1.9 Hz, 1H), 7.79 (m, 2H), 7.63 (m, 2H), 7.35 (m, 5H), 7.29 (d, J = 1.9 Hz, 1H), 3.71 (s, 3H), 1.85 (s, 6H). LCMS found, 419 $[M + H]^+$.

2-Methyl-2-(4-(3-methyl-2-oxo-8-(6-(trifluoromethyl)-pyridin-3-yl)-2,3-dihydro-1*H*-imidazo[4,5-*c*]quinolin-1-yl)-phenyl)propanenitrile (4d). Prepared from 2-(trifluorimethyl)-pyridin-5-ylboronic acid using General Procedure E. Purification was carried out by flash column chromatography over silica gel (eluent: CH_2Cl_2/MeOH 100:0 to 95:5) to give **4d** as a yellow-orange solid (yield: 25%). ^{1}H NMR (400 MHz, $CDCl_3$) δ ppm: 8.87 (s, 1H), 8.65 (s, 1H), 8.25 (d, J = 8.5 Hz, 1H), 7.80 (m, 5H), 7.71 (d, J = 8.1 Hz, 1H), 7.63 (d, J = 8.5 Hz, 2H), 3.73 (s, 3H), 1.86 (s, 6H). LCMS found, 488 $[M + H]^+$.

2-Methyl-2-(4-(3-methyl-8-(1-methyl-1*H*-pyrazol-4-yl)-2-oxo-2,3-dihydro-1*H*-imidazo[4,5-*c*]quinolin-1-yl)phenyl)-propanenitrile (4e). Prepared from 1-methylpyrazole-4-boronic acid pinacol ester using General Procedure E. Purification was carried out by flash column chromatography over silica gel (eluent: CH_2Cl_2/MeOH 100:0 to 95:5) to give **4e** as a yellow solid (yield: 49%). ^{1}H NMR (400 MHz, $CDCl_3$) δ ppm: 8.75 (s, 1H), 8.10 (d, J = 8.8 Hz, 1H), 7.81 (m, 2H), 7.68 (dd, J = 8.8 and 2.0 Hz, 2H), 7.63 (m, 2H), 7.41 (s, 1H), 7.34 (s, 1H), 7.14 (d, J = 1.78 Hz, 1H), 3.91 (s, 3H), 3.70 (s, 3H), 1.90 (s, 6H). LCMS found, 423 $[M + H]^+$.

2-(4-(8-(Benzo[b]thiophen-2-yl)-3-methyl-2-oxo-2,3-dihydro-1*H*-imidazo[4,5-*c*]quinolin-1-yl)phenyl)-2-methylpropanenitrile (4f). Prepared using General Procedure E, from **3**, providing **4f** as as an off-white solid (yield: 25%). ^{1}H NMR (400 MHz, $CDCl_3$) δ ppm: 8.79 (s, 1H), 8.14 (d, J = 9.1 Hz, 1H), 7.94 (dd, 9.1, J = 2.0 Hz, 1H), 7.86 (dd, J = 6.6, 2.0 Hz, 2H), 7.75 (m, 2H), 7.64 (dd, J = 6.6, 2.0 Hz, 2H), 7.44 (s, 1H), 7.37 (d, J = 1.8 Hz, 1H), 7.33 (m, 2H), 3.71 (s, 3H), 1.93 (s, 6H). LCMS found, 475 $[M + H]^+$.

2-Methyl-2-(4-(3-methyl-8-(4-methylpiperazin-1-yl)-2-oxo-2,3-dihydro-1*H*-imidazo[4,5-*c*]quinolin-1-yl)phenyl)-propanenitrile (5a). Prepared from intermediate **3** using General Procedure F. Purification was carried out by flash column chromatography over silica gel (eluent: CH_2Cl_2/MeOH 100:0 to 95:5) to give **5a** as a tan solid (yield: 17%). ^{1}H NMR (400 MHz, DMSO-d_6) δ ppm: 8.72 (s, 1H), 7.81 (m, 3H), 7.66 (d, J = 8.6 Hz, 2H), 7.39 (dd, J = 9.5, 2.5 Hz, 1H), 6.05 (d, J = 2.5 Hz, 1H), 3.54 (s, 3H), 2.82 (m, 4H), 2.31 (m, 4H), 2.16 (s, 3H), 1.78 (s, 6H). LCMS found, 441 $[M + H]^+$.

2-Methyl-2-(4-(3-methyl-8-morpholino-2-oxo-2,3-dihydro-1*H*-imidazo[4,5-*c*]quinolin-1-yl)phenyl)propanenitrile (5b). Prepared from **3** using General Procedure F, providing **5b** as a tan solid following flash column chromatography over silica gel (eluent: 0−3% MeOH/CH_2Cl_2) (yield: 12%). ^{1}H NMR (400 MHz, DMSO-d_6) δ ppm: 8.75 (s, 1H), 7.83 (m, 3H), 7.66 (d, J = 8.6 Hz, 2H), 7.40 (dd, J = 9.5, 2.5 Hz, 1H), 6.06 (d, J = 2.5 Hz, 1H), 3.61 (m, 4H), 3.55 (s, 3H), 2.77 (m, 4H), 1.78 (s, 6H). LCMS found, 428 $[M + H]^+$.

2-(4-(8-Amino-3-methyl-2-oxo-2,3-dihydro-1*H*-imidazo[4,5-*c*]quinolin-1-yl)phenyl)-2-methylpropanenitrile (6). A sealed vial was loaded with CuO (1 mg, 13 μmol), N^1,N^2-diisopropyloxalohydrazide[28] (10.2 mg, 51 μmol), intermediate **3** (120 mg, 0.25 mmol), commercial 25−28% aqueous ammonia solution (0.26 mL), K_3PO_4 (108 mg, 0.51 mmol), *tetra*-butyl ammonium bromide (41 mg, 0.13 mmol), and H_2O (0.26 mL). The mixture was heated at 110 °C for 3 h. After allowing the mixture to cool to rt, the reaction mixture was extracted with CH_2Cl_2 (3 × 10 mL). The combined organic phase was washed with brine and concentrated under vacuum. Purification was carried out by flash column chromatography over silica gel (eluent: CH_2Cl_2/MeOH 100:0 to 95:5) to give **6** as a white solid (18.4 mg, 51 μmol, 28%). ^{1}H NMR (400 MHz, DMSO-d_6) δ ppm: 8.58 (s, 1H), 7.74 (d, J = 8.6 Hz, 2H), 7.69 (d, J = 9.1 Hz, 1H), 7.54 (m, 2H), 6.94 (dd, J = 9.1, 2.3 Hz, 1H), 5.87 (d, J = 2.5 Hz, 1H), 5.39 (brs, 2H), 3.50 (s, 3H), 1.80 (s, 6H). LCMS found, 358 $[M + H]^+$.

***N*-(1-(4-(2-Cyanopropan-2-yl)phenyl)-3-methyl-2-oxo-2,3-dihydro-1*H*-imidazo[4,5-*c*]quinolin-8-yl)acetamide (7).** Acetyl chloride (10 μL, 0.14 mmol) was added to a mixture of compound **6** (50 mg, 0.14 mmol) and potassium carbonate (20 mg, 0.14 mmol) in CH_2Cl_2 (4 mL), and the resultant mixture was stirred for 24 h at rt. The mixture was filtered, and volatiles were removed under vacuum. Purification was carried out by flash column chromatography over silica gel (eluent: CH_2Cl_2/MeOH 100:0 to 93:7) to give **7** as a white solid (4.7 mg, 12 μmol, 8%). ^{1}H NMR (400 MHz, DMSO-d_6) δ ppm: 9.97 (s, 1H), 8.84 (s, 1H), 7.91 (d, J = 9.0 Hz, 1H), 7.79 (m, 1H), 7.74 (m, 2H), 7.55 (m, 2H), 7.33 (dd, J = 9.0, 2.6 Hz, 1H), 3.56 (s, 3H), 1.91 (s, 3H), 1.81 (s, 6H). LCMS found, 400 $[M + H]^+$.

2-(4-(3,8-Dimethyl-2-oxo-2,3-dihydro-1*H*-imidazo[4,5-*c*]-quinolin-1-yl)phenyl)-2-methylpropanenitrile (8). Prepared from intermediate **3** using General Procedure G. Compound **8** was obtained without further purification as an orange solid (yield: 90%, purity: 94%). ^{1}H NMR (400 MHz, DMSO-d_6) δ ppm: 8.93 (s, 1H), 7.92 (d, J = 8.8 Hz, 1H), 7.82 (d, J = 8.6 Hz, 2H), 7.66 (d, J = 8.3 Hz, 2H), 7.39 (dd, J = 8.8, 1.7 Hz, 1H), 6.64 (s, 1H), 3.58 (s, 3H), 2.16 (s, 3H), 1.82 (s, 6H). LCMS found, 357 $[M + H]^+$.

2-Methyl-2-(4-(3-methyl-2-oxo-2,3-dihydro-1*H*-imidazo[4,5-*c*]quinolin-1-yl)phenyl)propanenitrile (9). Prepared using General Procedure E, reacting intermediate **3** in the absence of boronic acid. Purification was carried out by flash column chromatography over silica gel (eluent: CH_2Cl_2/MeOH 100:0 to 95:5) to give **9** as a pale yellow solid (yield: 11%, purity: 93%). ^{1}H NMR (400 MHz, DMSO-d_6) δ ppm: 9.00 (s, 1H), 8.03 (d, J = 8.3 Hz, 1H), 7.8 (d, J = 8.6 Hz, 2H), 7.66 (d, J = 8.6 Hz, 2H), 7.55 (m, 1H), 7.31 (m, 1H), 7.03 (d, J = 7.8 Hz, 1H), 3.58 (s, 3H), 1.80 (s, 6H). LCMS found, 343 $[M + H]^+$.

2-(4-((6-Iodo-3-nitroquinolin-4-yl)amino)phenyl)-2-methylpropanenitrile (12). Prepared using General Procedure A, reacting intermediate **11** with 2-(4-amino-phenyl)-2-methylpropionitrile (Figure S2, Supporting Information). Compound **12** was isolated as a yellow solid (yield: 73%). ^{1}H NMR (400 MHz, DMSO-d_6) δ ppm: 10.1 (s, 1H), 9.10 (s, 1H), 8.80 (s, 1H), 8.12 (d, J = 8.6 Hz, 1H), 7.75 (d, J = 8.6 Hz, 1H), 7.46 (d, J = 8.6 Hz, 2H), 7.12 (d, J = 8.6 Hz, 2H), 1.67 (s, 6H). LCMS found, 459 $[M + H]^+$.

6-Iodo-3-nitro-*N*-(4-(trifluoromethyl)phenyl)quinolin-4-amine (12a). Prepared using General Procedure A, reacting intermediate **11** with 4-(trifluoromethyl) aniline. Compound **12a** was isolated as a yellow solid (yield: 78%). ^{1}H NMR (400 MHz, DMSO-d_6) δ ppm: 10.21 (s, 1H), 9.11 (s, 1H), 8.9 (s, 1H), 8.18 (d, J = 8.7 Hz 1H), 7.8 (d, J = 8.7 Hz, 1H), 7.65 (d, J = 8.3 Hz, 2H), 7.21 (d, J = 8.3 Hz, 2H). LCMS found, 458 $[M - H]^+$.

4-((6-Iodo-3-nitroquinolin-4-yl)amino)benzonitrile (12b). Prepared using the General Procedure A, reacting intermediate **11** with 4-aminobenzonitrile. Compound **12b** was isolated as a yellow solid (yield: 98%). ^{1}H NMR (400 MHz, DMSO-d_6) δ ppm: 10.36 (s, 1H), 9.11 (s, 1H), 8.85 (s, 1H), 8.16 (dd, J = 8.7, 1.8 Hz, 1H), 7.78 (d, J = 8.7 Hz, 1H), 7.72 (m, 2H), 7.12 (d, J = 8.6 Hz, 2H). LCMS found, 417 $[M + H]^+$.

6-Iodo-3-nitro-*N*-phenylquinolin-4-amine (12c). Prepared using General Procedure A, reacting intermediate **11** with aniline. Compound **12c** was isolated as a brown solid (yield: 83%). ^{1}H NMR (400 MHz, DMSO-d_6) δ ppm: 10.07 (s, 1H), 9.02 (s, 1H), 8.85 (d, J = 1.8 Hz, 1H), 8.11 (dd, J = 8.6, 1.6 Hz, 1H), 7.74 (d, J = 8.6 Hz, 1H), 7.32 (m, 2H), 7.13 (t, J = 7.3 Hz, 1H), 7.08 (d, J = 7.6 Hz, 2H). LCMS found, 392 $[M + H]^+$.

2-(4-((6-Iodo-3-nitroquinolin-4-yl)amino)phenyl)acetonitrile (12d). Prepared using General Procedure A, reacting intermediate **11** with 2-(4-aminophenyl)acetonitrile. Compound **12d** was isolated as a yellow solid (yield: 93%). ^{1}H NMR (400 MHz, DMSO-d_6) δ ppm: 10.06 (s, 1H), 9.04 (s, 1H), 8.93 (d, J = 1.8 Hz, 1H), 8.15 (dd, J = 8.7, 1.8 Hz, 1H), 7.77 (d, J = 8.7 Hz, 1H), 7.30 (d, J = 8.3 Hz, 2H), 7.10 (d, J = 8.3 Hz, 2H), 4.02 (s, 2H). LCMS found, 431 $[M + H]^+$.

6-Iodo-3-nitro-*N*-(*p*-tolyl)quinolin-4-amine (12e). Prepared using General Procedure A, reacting intermediate **11** with *p*-toluidine. Compound **12e** was isolated as a yellow solid (yield: 95%). ^{1}H NMR (400 MHz, DMSO-d_6) δ ppm: 10.03 (s, 1H), 9.01 (s, 1H), 8.87 (d, J = 1.6 Hz, 1H), 8.11 (dd, J = 8.6, 1.6 Hz, 1H), 7.73 (d, J = 8.6 Hz, 1H), 7.15 (d, J = 8.2 Hz, 2H), 6.99 (d, J = 8.2 Hz, 2H), 2.29 (s, 3H). LCMS found, 406 $[M + H]^+$.

6-Iodo-*N*-(4-methoxyphenyl)-3-nitroquinolin-4-amine (12g). Prepared using General Procedure A, reacting intermediate **11** with *p*-anisidine. Compound **12g** was isolated as an orange solid (yield: 83%). ^{1}H NMR (400 MHz, DMSO-d_6) δ ppm: 10.05 (s, 1H), 8.99 (s, 1H), 8.77 (s, 1H), 8.08 (dd, J = 8.7, 1.8 Hz, 1H), 7.70 (d, J = 8.7 Hz, 1H), 7.06 (d, J = 8.8 Hz, 2H), 6.91 (d, J = 8.8 Hz, 2H), 3.75 (s, 3H). LCMS found, 422 $[M + H]^+$.

N^1-(6-Iodo-3-nitroquinolin-4-yl)-N^4,N^4-dimethylbenzene-1,4-diamine (12h). Prepared using General Procedure A, reacting intermediate **11** with *N*,*N*-dimethyl *p*-phenylenediamine sulfate. Compound **12h** was isolated as an orange solid (yield: 92%).^{1}H NMR (400 MHz, DMSO-d_6) δ ppm: 10.14 (s, 1H), 9.00 (s, 1H), 8.73 (d, J = 1.5 Hz, 1H), 8.05 (dd, J = 8.7, 1.5 Hz, 1H), 7.68 (d, J = 8.7 Hz, 1H), 6.99 (d, J = 8.8 Hz, 2H), 6.70 (d, J = 8.8 Hz, 2H), 2.91 (s, 6H). LCMS found, 435 $[M + H]^+$.

6-Iodo-*N*-(4-morpholinophenyl)-3-nitroquinolin-4-amine (12i). Prepared using General Procedure A, reacting intermediate **11** with 4-morpholinoaniline. Compound **12i** was isolated as an orange solid (yield: 88%). ^{1}H NMR (400 MHz, DMSO-d_6) δ ppm: 10.09 (s, 1H), 9.01 (s, 1H), 8.72 (d, J = 1.8 Hz, 1H), 8.07 (dd, J = 8.8, 1.8 Hz, 1H), 7.70 (d, J = 8.8 Hz, 1H), 7.02 (d, J = 9.0 Hz, 2H), 6.93 (d, J = 9.0 Hz, 2H), 3.74 (t, J = 4.8 Hz, 4H), 3.11 (t, J = 4.8 Hz, 4H). LCMS found, 477 $[M + H]^+$.

6-Iodo-*N*-(4-((4-methylpiperazin-1-yl)methyl)phenyl)-3-nitroquinolin-4-amine (12j). Prepared using General Procedure A, reacting intermediate **11** with 4-[(4-methyl-1-piperazinyl)methyl]-aniline. Compound **12j** was isolated as a yellow solid (yield: 78%). ^{1}H NMR (400 MHz, $CDCl_3$) δ ppm: 10.69 (s, 1H), 9.45 (s, 1H), 7.89 (m, 2H), 7.70 (d, J = 9.3 Hz, 1H), 7.42 (d, J = 8.3 Hz, 2H), 7.14 (d, J = 8.3 Hz, 2H), 3.57 (s, 2H), 2.52 (m, 8H), 2.32 (s, 3H). LCMS found, 504 $[M + H]^+$.

6-Iodo-*N*-methyl-3-nitroquinolin-4-amine (12k). To a solution of intermediate **3** (1 g, 2.9 mmol) in MeOH (250 mL) was bubbled methylamine, and a precipitate was formed. The reaction mixture was stirred for another hour, after which the precipitate was recovered by filtration, washed with MeOH, and dried under vacuum to afford a yellow solid (0.7 g, 2.1 mmol, 74%). ^{1}H NMR (400 MHz, DMSO-d_6) δ ppm: 8.93 (s, 1H), 8.85 (m, 2H), 8.06 (dd, J = 8.8, 1.9 Hz, 1H), 7.64 (d, J = 8.8 Hz, 1H), 2.98 (s, 3H). LCMS found, 330 $[M + H]^+$.

2-(4-((3-Amino-6-iodoquinolin-4-yl)amino)phenyl)-2-methylpropanenitrile (13). Prepared from intermediate **12** using General Procedure B. Purification by flash column chromatography on silica gel (eluent: CH_2Cl_2/MeOH 100:0 to 95:5) gave **13** as a yellow solid (yield: 66%). ^{1}H NMR (400 MHz, CD_2Cl_2) δ ppm: 8.55 (s, 1H), 8.11 (s, 1H), 7.65 (m, 2H), 7.27 (d, J = 8.7 Hz, 2H), 6.60 (d, J = 8.7 Hz, 2H), 5.60 (brs, 1H), 4.04 (brs, 2H), 1.63 (s, 6H). LCMS found, 429 $[M + H]^+$.

6-Iodo-N^4-(4-(trifluoromethyl)phenyl)quinoline-3,4-diamine (13a). Prepared from intermediate **12a** using General Procedure B. Compound **13a** was isolated as a tan solid (yield: 94%). ^{1}H NMR (400 MHz, DMSO-d_6) δ ppm: 8.62 (s, 1H), 8.35 (s, 1H), 8.01 (s, 1H), 7.61 (s, 2H), 7.44 (d, J = 8.2 Hz, 2H), 6.59 (d, J = 8.2 Hz, 2H), 5.55 (brs, 2H). LCMS found 43,0 $[M + H]^+$.

4-((3-Amino-6-iodoquinolin-4-yl)amino)benzonitrile (13b). Prepared from intermediate **12b** using the General Procedure B. Compound **13b** was isolated as a tan solid (yield: 84%). ^{1}H NMR (400 MHz, DMSO-d_6) δ ppm: 8.61 (s, 1H), 8.56 (s, 1H), 7.96 (s, 1H), 7.61 (m, 2H), 7.52 (d, J = 8.8 Hz, 2H), 6.56 (m, 2H), 5.62 (s, 2H). LCMS found, 387 $[M + H]^+$.

6-Iodo-N^4-phenylquinoline-3,4-diamine (13c). Prepared from **12c** using General Procedure B. Compound **13c** was isolated as a tan solid (yield: 98%). ^{1}H NMR (400 MHz, DMSO-d_6) δ ppm: 8.58 (s, 1H), 8.05 (s, 1H), 7.81 (s, 1H), 7.59 (d, J = 1.01 Hz, 2H), 7.12 (dd, J = 7.3, 1.0 Hz, 2H), 6.69 (t, J = 7.3 Hz, 1H), 6.51 (m, 2H), 1.89 (brs, 2H). LCMS found, 360 $[M - H]^+$.

2-(4-((3-Amino-6-iodoquinolin-4-yl)amino)phenyl)-acetonitrile (13d). Prepared from intermediate using General Procedure B. Compound **13d** was isolated as a tan solid (yield: 87%). ^{1}H NMR (400 MHz, DMSO-d_6) δ ppm: 8.60 (s, 1H), 8.05 (s,1H), 7.91 (s, 1H), 7.60 (m, 2H), 7.10 (d, J = 8.4 Hz, 2H), 6.52 (d, J = 8.4 Hz, 2H), 5.40 (s, 2H), 3.85 (s, 2H). LCMS found, 401 $[M + H]^+$.

6-Iodo-N^4-(*p*-tolyl)quinoline-3,4-diamine (13e). Prepared from intermediate **12e** using General Procedure B. Compound **13e** was isolated as a yellow solid (yield: 30%). ^{1}H NMR (400 MHz, DMSO-d_6) δ ppm: 8.55 (s, 1H), 8.25 (d, J = 1.5 Hz, 1H), 7.83 (dd, J = 8.8, 1.5 Hz, 1H), 7.70 (d, J = 8.8 Hz, 1H), 7.09 (d, J = 8.2 Hz, 2H), 6.72 (d, J = 8.2 Hz, 2H), 5.44 (brs, 2H), 2.26 (s, 3H). LCMS found, 376 $[M - H]^+$.

6-Iodo-N^4-(4-methoxyphenyl)quinoline-3,4-diamine (13g). Prepared from intermediate **12g** using General Procedure B. Compound **13g** was obtained as a tan solid (yield: 37%). ^{1}H NMR (400 MHz, DMSO-d_6) δ ppm: 8.55 (s, 1H), 8.09 (m, 1H), 7.56 (m, 3H), 6.75 (d, J = 9.0 Hz, 2H), 6.48 (d, J = 9.0 Hz, 2H), 5.25 (brs, 2H), 3.64 (s, 3H). LCMS found, 392 $[M + H]^+$.

N^4-(4-(Dimethylamino)phenyl)-6-iodoquinoline-3,4-diamine (13h). Prepared from intermediate **12h** using General Procedure B. Compound **13h** was isolated as an orange solid (yield: 84%). ^{1}H NMR (400 MHz, DMSO-d_6) δ ppm: 8.53 (s, 1H), 8.13 (s,1H), 7.58 (d, J = 1.5 Hz, 2H), 7.47 (s, 1H), 6.65 (d, J = 9.0 Hz, 2H), 6.49 (d, J = 9.0 Hz, 2H), 5.18 (s, 2H), 2.76 (s, 6H). LCMS found, 405 $[M + H]^+$.

6-Iodo-N^4-(4-morpholinophenyl)quinoline-3,4-diamine (13i). Prepared from intermediate **12i** using General Procedure B. Purification of the crude was carried out by recrystallization from EtOH/Et_2O to give **13i** as a yellow solid (yield: 45%). ^{1}H NMR (400 MHz, DMSO-d_6) δ ppm: 8.56 (s, 1H), 8.11 (s,1H), 7.57 (m, 3H), 6.80 (d, J = 8.8 Hz, 2H), 6.48 (d, J = 8.8 Hz, 2H), 6.24 (brs, 2H), 3.70 (t, J = 4.7 Hz, 4H), 2.93 (t, J = 4.7 Hz, 4H). LCMS found, 447 $[M + H]^+$.

6-Iodo-N^4-(4-((4-methylpiperazin-1-yl)methyl)phenyl)-quinoline-3,4-diamine (13j). Prepared from intermediate **12j** using General Procedure B. Compound **13j** was isolated as an off-white solid (yield: 66%). ^{1}H NMR (400 MHz, DMSO-d_6) δ ppm: 8.59 (s, 1H), 8.06 (s, 1H), 7.78 (s, 1H), 7.59 (m, 2H), 7.03 (d, J = 8.5 Hz, 2H), 6.48 (d, J = 8.5 Hz, 2H), 5.34 (s, 2H), 3.29 (s, 2H), 2.30 (m, 8H), 2.12 (s, 3H). LCMS found, 472 $[M - H]^+$.

6-Iodo-N^4-methylquinoline-3,4-diamine (13k). Prepared from intermediate **12k** using General Procedure B. Purification of the crude was carried out by recrystallization from Et_2O to give **13k** as a yellow gummy solid (yield: 49%). ^{1}H NMR (400 MHz, $CDCl_3$) δ ppm: 8.46 (s, 1H), 8.20 (s, 1H), 7.68 (m, 2H), 4.30 (s, 1H), 3.82 (brs, 2H), 2.99 (s, 3H). LCMS found, 300 $[M + H]^+$.

2-(4-(8-Iodo-2-oxo-2,3-dihydro-1*H*-imidazo[4,5-*c*]quinolin-1-yl)phenyl)-2-methylpropanenitrile (14). Prepared from **13** using General Procedure C to give **14** as a brown solid (yield: 91%). ^{1}H NMR (400 MHz, DMSO-d_6) δ ppm: 8.77 (s, 1H), 7.83 (d, J = 8.5 Hz, 2H), 7.74 (m, 2H), 7.67 (d, J = 8.5 Hz, 2H), 7.14 (s, 1H), 5.74 (s, 1H), 1.79 (s, 6H). LCMS found, 455 $[M + H]^+$.

8-Iodo-1-(4-(trifluoromethyl)phenyl)-1*H*-imidazo[4,5-*c*]-quinolin-2(3*H*)-one (14a). Prepared from intermediate **13a**, using General Procedure C. Compound **14a** was isolated as a white solid (yield: 91%). ^{1}H NMR (400 MHz, DMSO-d_6) δ ppm: 8.73 (s, 1H), 8.03 (d, J = 7.9 Hz, 2H), 7.82 (d, J = 7.9 Hz, 2H), 7.71 (m, 2H), 7.29 (s, 1H), 3.35 (brs, 1H). LCMS found, 454 $[M - H]^+$.

4-(8-Iodo-2-oxo-2,3-dihydro-1*H*-imidazo[4,5-*c*]quinolin-1-yl)benzonitrile (14b). Prepared from intermediate **13b** using the General Procedure C. Compound **14b** was isolated as a yellow solid (yield: 99%). ^{1}H NMR (400 MHz, DMSO-d_6) δ ppm: 8.68 (s, 1H), 8.1 (d, J = 8.6 Hz, 2H), 7.76 (m, 2H), 7.68 (s, 1H), 7.36 (d, J = 1.8 Hz, 1H), 6.58 (d, J = 8.6 Hz, 1H), 6.12 (brs, 1H). LCMS found, 413 $[M + H]^+$.

8-Iodo-1-phenyl-1*H*-imidazo[4,5-*c*]quinolin-2(3*H*)-one (14c). Prepared from intermediate **13c** using General Procedure C.

dx.doi.org/10.1021/jm500361r | J. Med. Chem. 2014, 57, 4834−4848

Compound **14c** was isolated as a white solid (yield: 94%). ^{1}H NMR (400 MHz, DMSO-d_6) δ ppm: 8.76 (s, 1H), 7.75 (m, 2H), 7. 67 (m, 3H), 7.60 (m, 2H), 7.27 (m, 2H). LCMS found, 386 $[M - H]^+$.

2-(4-(8-Iodo-2-oxo-2,3-dihydro-1*H*-imidazo[4,5-*c*]quinolin-1-yl)phenyl)acetonitrile. (14d). Prepared from intermediate **13d** using General Procedure C. Compound **14d** was isolated as a yellow brown solid (yield: 62%). ^{1}H NMR (400 MHz, DMSO-d_6) δ ppm: 8.68 (s, 1H), 7.76 (s, 1H), 7.69 (d, J = 8.8 Hz, 1H), 7.62 (m, 3H), 7.54 (d, J = 8.6 Hz, 2H), 7.40 (d, J = 1.5 Hz, 1H), 4.23 (s, 2H). LCMS found, 427 $[M + H]^+$

8-Iodo-1-(*p*-tolyl)-1*H*-imidazo[4,5-*c*]quinolin-2(3*H*)-one (14e). Prepared from intermediate **13e** using General Procedure C. Compound **14e** was isolated as a tan solid (yield: 82%). ^{1}H NMR (400 MHz, DMSO-d_6) δ ppm: 8.70 (s, 1H), 7.69 (m, 2H), 7.44 (m, 6H), 2.47 (s, 3H). LCMS found, 402 $[M + H]^+$.

8-Iodo-1-(4-methoxyphenyl)-1*H*-imidazo[4,5-*c*]quinolin-2(3*H*)-one (14g). Prepared from intermediate **13g** using General Procedure C. Compound **14g** was obtained as a tan solid (yield: 79%). ^{1}H NMR (400 MHz, DMSO-d_6) δ ppm: 8.71 (s, 1H), 7.70 (m, 2H), 7.46 (d, J = 8.8 Hz, 2H), 7.35 (d, J = 1.0 Hz, 1H), 7.19 (d, J = 8.8 Hz, 2H), 3.87 (s, 3H), 3.55 (brs, 1H). LCMS found, 418 $[M + H]^+$.

1-(4-(Dimethylamino)phenyl)-8-iodo-1*H*-imidazo[4,5-*c*]-quinolin-2(3*H*)-one (14h). Prepared from intermediate **13h** using General Procedure C. Compound **14h** was isolated as a brown solid (yield: 57%). ^{1}H NMR (400 MHz, DMSO-d_6) δ ppm: 8.73 (s, 1H), 7.74 (m, 2H), 7.44 (m, 1H), 7.32 (d, J = 8.9 Hz, 2H), 6.93 (d, J = 8.9 Hz, 2H), 3.33 (brs, 1H), 3.02 (s, 6H). LCMS found, 431 $[M + H]^+$.

8-Iodo-1-(4-morpholinophenyl)-1*H*-imidazo[4,5-*c*]quinolin-2(3*H*)-one (14i). Prepared from intermediate **13i** using General Procedure C. Compound **14i** was isolated as a brown solid (yield: 39%). ^{1}H NMR (400 MHz, DMSO-d_6) δ ppm: 8.64 (s, 1H), 7.66 (d, J = 8.8 Hz, 1H), 7.60 (d, J = 8.8 Hz, 1H), 7.40 (d, J = 1.8 Hz, 1H), 7.32 (d, J = 8.7 Hz, 2H), 7.16 (d, J = 8.7 Hz, 2H), 3.80 (t, J = 4.7 Hz, 4H), 3.37 (brs, 1H), 3.23 (t, J = 4.7 Hz, 4H). LCMS found, 473 $[M + H]^+$.

8-Iodo-1-(4-((4-methylpiperazin-1-yl)methyl)phenyl)-1*H*-imidazo[4,5-*c*]quinolin-2(3*H*)-one (14j). Prepared from intermediate **13j** using General Procedure C. Compound **14j** was isolated as a yellow solid (yield: 87%). ^{1}H NMR (400 MHz, DMSO-d_6) δ ppm: 8.76 (s, 1H), 7.75 (m, 2H), 7.59 (d, J = 8.1 Hz, 2H), 7.53 (d, J = 8.1 Hz, 2H), 7.20 (s, 1H), 3.61 (s, 2H), 2.36 (m, 9H), 2.16 (s, 3H). LCMS found, 500 $[M + H]^+$.

8-Iodo-1-methyl-1*H*-imidazo[4,5-*c*]quinolin-2(3*H*)-one (14k). Prepared from intermediate **13k** using General Procedure C. Compound **14k** was isolated as a yellow solid (yield: 98%). ^{1}H NMR (400 MHz, DMSO-d_6) δ ppm: 8.54 (s, 1H), 8.51 (d, 1.0 Hz, 1H), 7.64 (m, 2H), 3.71 (s, 3H), 3.18 (brs, 1H). LCMS found, 326 $[M + H]^+$.

8-Iodo-3-methyl-1-(4-(trifluoromethyl)phenyl)-1*H*-imidazo-[4,5-*c*]quinolin-2(3*H*)-one (15a). Prepared from intermediate **14a** using General Procedure D. Compound **15a** was isolated as a pale yellow solid (yield: 75%). ^{1}H NMR (400 MHz, DMSO-d_6) δ ppm: 9.01 (s, 1H), 7.77 (m, 1H), 7.69 (m, 3H), 7.60 (m, 2H), 7.27 (m, 1H), 3.57 (s, 3H). LCMS found, 468 $[M - H]^+$.

4-(8-Iodo-3-methyl-2-oxo-2,3-dihydro-1*H*-imidazo[4,5-*c*]-quinolin-1-yl)benzonitrile (15b). Prepared from intermediate **14b** using General Procedure D. Compound **15b** was isolated as a yellow solid (yield: 57%). ^{1}H NMR (400 MHz, DMSO-d_6) δ ppm: 9.05 (s, 1H), 8.20 (d, J = 8.6 Hz, 2H), 7.87 (d, J = 8.6 Hz, 2H), 7.81 (m, 2H), 7.30 (m, 1H), 3.58 (s, 3H). LCMS found, 427 $[M + H]^+$.

8-Iodo-3-methyl-1-phenyl-1*H*-imidazo[4,5-*c*]quinolin-2(3*H*)-one (15c). Prepared from intermediate **14c** using General Procedure D. Compound **15c** was isolated as a pale yellow solid (yield: 44%). ^{1}H NMR (400 MHz, DMSO-d_6) δ ppm: 9.01 (s, 1H), 7.77 (m, 2H), 7.69 (m, 2H), 7.60 (m, 2H), 7.27 (m, 2H), 3.58 (s, 3H). LCMS found, 402 $[M + H]^+$.

2-(4-(8-Iodo-3-methyl-2-oxo-2,3-dihydro-1*H*-imidazo[4,5-*c*]-quinolin-1-yl)phenyl)acetonitrile (15d). To a solution of **14d** (0.4 g, 0.94 mmol) in DMF (25 mL) were successively added K_2CO_3 (156 mg, 1.13 mmol) and methyl iodide (70 μL, 1.13 mmol). The resultant mixture was stirred for 4.5 h at rt and then filtered. Volatiles were evaporated under reduced pressure to give a precipitate that was washed with H_2O and dried under vacuum to afford **15d** (0.37 g, 0.84 mmol, 90%) as a purple solid. ^{1}H NMR (400 MHz, DMSO-d_6) δ ppm: 9.03 (s, 1H), 7.80 (m, 2H), 7.66 (m, 4H), 7.36 (s, 1H), 4.27 (s, 2H), 3.59 (s, 3H). LCMS found, 441 $[M + H]^+$.

8-Iodo-3-methyl-1-(*p*-tolyl)-1*H*-imidazo[4,5-*c*]quinolin-2(3*H*)-one (15e). Prepared from intermediate **14e** using General Procedure D. Compound **15e** was isolated as a brown solid (yield: 93%). ^{1}H NMR (400 MHz, DMSO-d_6) δ ppm: 9.01 (s, 1H), 7.78 (d, J = 1.5 Hz, 2H), 7.48 (m, 4H), 7.36 (m, 1H), 3.58 (s, 3H), 3.31 (s, 3H). LCMS found, 416 $[M + H]^+$.

8-Iodo-1-(4-methoxyphenyl)-3-methyl-1*H*-imidazo[4,5-*c*]-quinolin-2(3*H*)-one (15g). Prepared from intermediate **14g** using General Procedure D. Compound **15g** was obtained as a tan solid (yield: 73%). ^{1}H NMR (400 MHz, DMSO-d_6) δ ppm: 8.09 (s, 1H), 7.77 (m, 2H), 7.50 (d, J = 9.0 Hz, 2H), 7.35 (m, 1H), 7.21 (d, J = 9.0 Hz, 2H), 3.88 (s, 3H), 3.57 (s, 3H). LCMS found, 432 $[M + H]^+$.

1-(4-(Dimethylamino)phenyl)-8-iodo-3-methyl-1*H*-imidazo-[4,5-*c*]quinolin-2(3*H*)-one (15h). Prepared from intermediate **14h** using General Procedure D. Compound **15h** was isolated as a brown solid (yield: 70%). ^{1}H NMR (400 MHz, DMSO-d_6) δ ppm: 8.98 (s, 1H), 7.77 (m, 2H), 7.45 (m, 1H), 7.33 (d, J = 9.0 Hz, 2H), 6.93 (d, J = 9.0 Hz, 2H), 3.57 (s, 3H), 3.03 (s, 6H). LCMS found, 445 $[M + H]^+$.

8-Iodo-3-methyl-1-(4-morpholinophenyl)-1*H*-imidazo[4,5-*c*]quinolin-2(3*H*)-one (15i). Prepared from intermediate **14i** using General Procedure D. Compound **15i** was isolated as a brown solid (yield: 76%). ^{1}H NMR (400 MHz, DMSO-d_6) δ ppm: 8.99 (s, 1H), 7.78 (m, 2H), 7.41 (m, 3H), 7.20 (d, J = 9.1 Hz, 2H), 3.81 (t, J = 4.8 Hz, 4H), 3.57 (s, 3H), 3.27 (t, J = 4.8 Hz, 4H). LCMS found, 487 $[M + H]^+$.

8-Iodo-1,3-dimethyl-1*H*-imidazo[4,5-*c*]quinolin-2(3*H*)-one (15k). A mixture of intermediate **14k** (53 mg, 0.16 mmol), K_2CO_3 (34 mg, 0.24 mmol), and methyl iodide (15 μL, 0.24 mmol) in acetone (15 mL) was stirred for 17 h at rt. To complete the reaction another equiv of K_2CO_3 (24 mg, 0.16 mmol) and methyl iodide (10 μL, 0.16 mmol) were added, and the resultant solution was left under stirring for 48 h. The mixture was then taken to dryness, and the solids were washed with H_2O to give **15k** as a yellow solid (23 mg, 68 μmol, 42%). ^{1}H NMR (400 MHz, DMSO-d_6) δ ppm: 8.89 (s, 1H), 8.60 (d, J = 1.8 Hz, 1H), 7.87 (dd, J = 8.8, 1.8 Hz, 1H), 7.79 (d, J = 8.8 Hz, 1H), 3.80 (s, 3H), 3.52 (s, 3H). LCMS found, 340 $[M + H]^+$.

3-Methyl-8-(quinolin-3-yl)-1-(4-(trifluoromethyl)phenyl)-1*H*-imidazo[4,5-*c*]quinolin-2(3*H*)-one (16a). Prepared using General Procedure E, reacting intermediate **15a** with 3-quinoline boronic acid. Purification was carried out by flash column chromatography over silica gel (eluent: CH_2Cl_2/MeOH 100:0 to 95:5) to give **16a** as a yellow solid (yield: 26%). ^{1}H NMR (400 MHz, DMSO-d_6) δ ppm: 9.08 (s, 1H), 8.92 (d, J = 2.3 Hz, 1H), 8.26 (d, J = 2.0 Hz, 1H), 8.21 (d, J = 8.8 Hz, 1H), 8.14 (m, 3H), 8.03 (d, J = 8.6 Hz, 1H), 7.99 (d, J = 8.1 Hz, 2H), 7.92 (d, J = 7.3 Hz, 1H), 7.77 (m, 1H), 7.66 (m, 1H), 7.33 (d, J = 1.8 Hz, 1H), 3.63 (s, 3H). LCMS found, 471 $[M + H]^+$.

4-(3-Methyl-2-oxo-8-(quinolin-3-yl)-2,3-dihydro-1*H*-imidazo[4,5-*c*]quinolin-1-yl)benzonitrile (16b). Prepared using General Procedure E, reacting intermediate **15b** with 3-quinoline boronic acid. Purification was carried out by flash column chromatography over silica gel (eluent: CH_2Cl_2/MeOH 100:0 to 95:5) to give **16b** as a pale yellow solid (yield: 43%). ^{1}H NMR (400 MHz, DMSO-d_6) δ ppm: 9.08 (s, 1H), 8.90 (d, J = 2.5 Hz, 1H), 8.37 (d, J = 2.3 Hz, 1H), 8.26 (d, J = 8.6 Hz, 2H), 8.21 (m, 1H), 8.12 (dd, J = 9.1, 2.0 Hz, 1H), 8.03 (m, 2H), 7.97 (m, 2H), 7.79 (m, 1H), 7.67 (m, 1H), 7.35 (d, J = 1.8 Hz, 1H), 3.62 (s, 3H). LCMS found, 428 $[M + H]^+$.

3-Methyl-1-phenyl-8-(quinolin-3-yl)-1*H*-imidazo[4,5-*c*]-quinolin-2(3*H*)-one (16c). Prepared using General Procedure E, reacting intermediate **15c** with 3-quinoline boronic acid. Purification was carried out by flash column chromatography over silica gel (eluent: CH_2Cl_2/MeOH 100:0 to 95:5) to give **16c** as a white solid (yield: 38%). ^{1}H NMR (400 MHz, DMSO-d_6) δ ppm: 9.04 (s, 1H), 8.79 (d, J = 2.3 Hz, 1H), 8.37 (d, J = 2.3 Hz, 1H), 8.18 (d, J = 8.8 Hz, 1H), 8.10 (dd, J = 8.8, 2.0 Hz, 1H), 8.03 (d, J = 8.3 Hz, 1H), 7.98 (d, J = 7.3 Hz, 1H), 7.74 (m, 6H), 7.66 (m, 1H), 7.35 (d, J = 1.8 Hz, 1H),3.62 (s, 3H). LCMS found, 403 $[M + H]^+$.

dx.doi.org/10.1021/jm500361r | *J. Med. Chem.* 2014, 57, 4834−4848

2-(4-(3-Methyl-2-oxo-8-(pyridin-4-yl)-2,3-dihydro-1*H*-imidazo[4,5-*c*]quinolin-1-yl)phenyl)acetonitrile (16d). Prepared using General Procedure E, reacting intermediate **15d** with pyridine 4-boronic acid pinacol ester. Purification was carried out by flash column chromatography over silica gel (eluent: CH_2Cl_2/MeOH 100:0 to 95:5) to give **16d** as a yellow solid (yield: 17%). ^{1}H NMR (400 MHz, DMSO-d_6) δ ppm: 9.05 (s, 1H), 8.60 (d, J = 5.0 Hz, 2H), 8.15 (d, J = 8.6 Hz, 1H), 8.00 (d, J = 8.08 Hz, 1H), 7.73 (m, 4H), 7.30 (m, 3H), 4.28 (s, 2H), 3.61 (s, 3H). LCMS found, 392 $[M + H]^+$.

3-Methyl-8-(pyridin-4-yl)-1-(*p*-tolyl)-1*H*-imidazo[4,5-*c*]quinolin-2(3*H*)-one (16e). Prepared using General Procedure E, reacting intermediate **15e** with pyridine 4-boronic acid pinacol ester. Purification was carried out by flash column chromatography over silica gel (eluent: CH_2Cl_2/MeOH 100:0 to 90:10) to give **16e** as a yellow solid (yield: 54%). ^{1}H NMR (400 MHz, DMSO-d_6) δ ppm: 9.04 (s, 1H), 8.59 (dd, J = 4.5, 1.9 Hz, 2H), 8.14 (d, J = 8.8 Hz, 1H), 7.98 (dd, J = 8.8, 1.9 Hz, 1H), 7.55 (m, 4H), 7.31 (dd, J = 4.5, 1.5 Hz, 2H), 7.25 (d, J = 2.0 Hz, 1H), 3.61 (s, 3H), 3.31 (s, 3H). LCMS found, 367 $[M + H]^+$.

4-(3-Methyl-2-oxo-8-(pyridin-4-yl)-2,3-dihydro-1*H*-imidazo-[4,5-*c*]quinolin-1-yl)benzonitrile (16f). Prepared using General Procedure E, reacting intermediate **15b** with pyridine 4-boronic acid pinacol ester. Purification was carried out by flash column chromatography over silica gel (eluent: CH_2Cl_2/MeOH 100:0 to 95:5) to give **16f** as a white solid (yield: 5%). ^{1}H NMR (400 MHz, DMSO-d_6) δ ppm: 9.08 (s, 1H), 8.59 (d, J = 6.3 Hz, 2H), 8.22 (d, J = 8.6 Hz, 2H), 8.17 (d, J = 9.1 Hz, 1H), 7.98 (dd, J = 9.1, 2.0 Hz, 1H), 7.94 (d, J = 8.6 Hz, 2H), 7.35 (d, J = 6.3 Hz, 2H), 7.29 (d, J = 2.0 Hz, 1H), 3.61 (s, 3H). LCMS found, 428 $[M + H]^+$.

1-(4-Methoxyphenyl)-3-methyl-8-(pyridin-4-yl)-1*H*-imidazo-[4,5-*c*]quinolin-2(3*H*)-one (16g). Prepared using General Procedure E, reacting intermediate **15g** with pyridine 4-boronic acid pinacol ester. Purification was carried out by flash column chromatography over silica gel (eluent: CH_2Cl_2/MeOH 100:0 to 95:5) to give **16g** as a tan solid (yield: 32%). ^{1}H NMR (400 MHz, DMSO-d_6) δ ppm: 9.02 (s, 1H), 8.57 (m, 2H), 8.13 (d, J = 8.8 Hz, 1H), 7.96 (dd, J = 8.8, 2.0 Hz, 1H), 7.58 (d, J = 8.8 Hz, 2H), 7.34 (m, 2H), 7.30 (d, J = 2.0 Hz, 1H), 7.26 (m, 2H), 3.92 (s, 3H), 3.60 (s, 3H). LCMS found, 383 $[M + H]^+$.

1-(4-(Dimethylamino)phenyl)-3-methyl-8-(pyridin-4-yl)-1*H*-imidazo[4,5-*c*]quinolin-2(3*H*)-one (16h). Prepared using General Procedure E, reacting intermediate **15h** with pyridine 4-boronic acid pinacol ester. Purification was carried out by flash column chromatography over silica gel (eluent: CH_2Cl_2/MeOH 100:0 to 90:10) to give **16h** as a salmon solid (yield: 16%). ^{1}H NMR (400 MHz, DMSO-d_6) δ ppm: 9.00 (s, 1H), 8.56 (d, J = 5.8 Hz, 2H), 8.12 (d, J = 8.8 Hz, 1H), 7.98 (dd, J = 8.4, 1.78 Hz, 1H), 7.38 (m, 5H), 6.99 (d, J = 8.8 Hz, 2H), 3.60 (s, 3H), 3.06 (s, 6H). LCMS found, 396 $[M + H]^+$.

3-Methyl-1-(4-morpholinophenyl)-8-(pyridin-4-yl)-1*H*-imidazo[4,5-*c*]quinolin-2(3*H*)-one (16i). Prepared using General Procedure E, reacting intermediate **15i** with pyridine 4-boronic acid pinacol ester. Purification was carried out by flash column chromatography over silica gel (eluent: CH_2Cl_2/MeOH 100:0 to 90:10) to give **16i** as a salmon solid (yield: 28%). ^{1}H NMR (400 MHz, DMSO-d_6) δ ppm: 9.02 (s, 1H), 8.58 (d, J = 5.8 Hz, 2H), 8.13 (d, J = 8.8 Hz, 1H), 7.99 (dd, J = 8.8, 1.9 Hz, 1H), 7.49 (d, J = 8.8 Hz, 2H), 7.37 (m, 3H), 7.25 (d, J = 8.8 Hz, 2H), 3.83 (m, 4H), 3.61 (s, 3H), 3.24 (m, 4H). LCMS found, 438 $[M + H]^+$.

1-(4-((4-Methylpiperazin-1-yl)methyl)phenyl)-8-(pyridin-4-yl)-1*H*-imidazo[4,5-*c*]quinolin-2(3*H*)-one (16j). Prepared using General Procedure E, reacting intermediate **14j** with pyridine 4-boronic acid pinacol ester. Purification was carried out by flash column chromatography over amino-silica gel (eluent: CH_2Cl_2/MeOH 100:0 to 95:5) to give **16j** as a white solid (yield: 23%). ^{1}H NMR (400 MHz, DMSO-d_6) δ ppm: 8.78 (s, 1H), 8.54 (m, 2H), 8.10 (d, J = 9.1 Hz, 1H), 7.91 (dd, J = 8.8, 1.9 Hz, 1H), 7.60 (m, 3H), 7.52 (m, 2H), 7.36 (d, J = 1.9 Hz, 1H), 7.31 (dd, J = 4.4, 1.6 Hz, 2H), 3.65 (s, 2H), 2.45 (m, 4H), 2.33 (m, 4H), 2.17 (s, 3H). LCMS found, 451 $[M + H]^+$.

1-Methyl-8-(pyridin-4-yl)-1*H*-imidazo[4,5-*c*]quinolin-2(3*H*)-one (16k). Prepared using General Procedure E, reacting intermediate **15k** with pyridine 4-boronic acid pinacol ester. Purification was carried out by flash column chromatography over silica gel (eluent: CH_2Cl_2/MeOH 100:0 to 90:10) to give **16k** as a yellow solid (yield: 20%). ^{1}H NMR (400 MHz, $CDCl_3$) δ ppm: 8.76 (m, 3H), 8.51 (d, J = 1.7 Hz, 1H), 8.28 (d, J = 8.8 Hz, 1H), 7.90 (dd, J = 8.8, 1.7 Hz, 1H), 7.64 (dd, J = 4.5, 1.6, 2H), 4.03 (s, 3H), 3.66 (s, 3H). LCMS found, 291 $[M + H]^+$.

4-(2-Oxo-8-(quinolin-3-yl)-2,3-dihydro-1*H*-imidazo[4,5-*c*]-quinolin-1-yl)benzonitrile (17b). Prepared using General Procedure E, reacting intermediate **14b** with 3-quinoline boronic acid. Purification was carried out by flash column chromatography over silica gel (eluent: CH_2Cl_2/MeOH 100:0 to 95:5) to give **17b** as a white solid (yield: 43%). ^{1}H NMR (400 MHz, DMSO-d_6) δ ppm: 8.90 (d, J = 2.3 Hz, 1H), 8.81 (s, 1H), 8.37 (d, J = 2.0 Hz, 1H), 8.23 (d, J = 8.6 Hz, 2H), 8.18 (d, J = 8.8 Hz, 1H), 8.04 (m, 3H), 7.96 (d, J = 8.6 Hz, 2H), 7.78 (m, 1H), 7.66 (m, 1H), 7.38 (d, J = 2.0 Hz, 1H), 5.95 (s, 1H). LCMS found, 414 $[M + H]^+$.

2-(4-(2-Oxo-8-(pyridin-4-yl)-2,3-dihydro-1*H*-imidazo[4,5-*c*]-quinolin-1-yl)phenyl)acetonitrile (17d). Prepared using General Procedure E, reacting intermediate **14d** with 4-pyridine boronic ester. Purification was carried out by flash column chromatography over silica gel (eluent: CH_2Cl_2/MeOH 100:0 to 95:5) to give **17d** as a yellow solid (yield: 12%). ^{1}H NMR (400 MHz, DMSO-d_6) δ ppm: 8.81 (s, 1H), 8.59 (dd, J = 4.5, 1.7 Hz, 2H), 8.12 (d, J = 8.9 Hz, 1H), 7.99 (dd, J = 8.9, 2.0 Hz, 1H), 7.72 (m, 4H), 7.31 (dd, J = 4.5, 1.7 Hz, 2H), 7.29 (d, J = 2.0 Hz, 1H), 4.28 (s, 2H), 3.33 (brs, 1H). LCMS found, 378 $[M + H]^+$.

1-(4-(Dimethylamino)phenyl)-8-(pyridin-4-yl)-1*H*-imidazo-[4,5-*c*]quinolin-2(3H)-one (17h). Prepared using General Procedure E, reacting intermediate **14h** with pyridine 4-boronic acid pinacol ester. Purification was carried out by flash column chromatography over silica gel (eluent: CH_2Cl_2/MeOH 100:0 to 90:10) to give **17h** as a salmon solid (yield: 9%, purity: 94%). ^{1}H NMR (400 MHz, DMSO-d_6) δ ppm: 8.76 (s, 1H), 8.56 (d, J = 5.8 Hz, 2H), 8.09 (d, J = 8.8 Hz, 1H), 7.97 (dd, J = 8.8, 2.0 Hz, 1H), 7.38 (m, 6H), 6.99 (d, J = 9.1 Hz, 2H), 3.06 (s, 6H). LCMS found, 382 $[M + H]^+$. Also isolated from this reaction was 1-(4-(dimethylamino)phenyl)-1*H*-imidazo[4,5-*c*]-quinolin-2(3*H*)-one M1009/84/4. (**18**) (yield: 5%). ^{1}H NMR (400 MHz, DMSO-d_6) δ ppm: 8.72 (s, 1H), 7.98 (d, J = 8.3 Hz, 1H), 7.47 (m, 2H), 7.31 (m, 3H), 7.15 (d, J = 8.3 Hz, 1H), 6.89 (d, J = 8.8 Hz, 2H), 3.02 (s, 6H). LCMS found, 305 $[M + H]^+$.

1-(4-(Dimethylamino)phenyl)-3-methyl-1*H*-imidazo[4,5-*c*]-quinolin-2(3*H*)-one (19). Prepared using the General Procedure E, reacting intermediate **15h** in the absence of boronic acid. Purification was carried out by flash column chromatography over silica gel (eluent: CH_2Cl_2/MeOH 100:0 to 95:5) to give **19** as a salmon solid. (yield: 13%, purity: 91%). ^{1}H NMR (400 MHz, DMSO-d_6) δ ppm: 8.96 (s, 1H), 8.01 (d, J = 8.3 Hz, 1H), 7.56 (m, 1H), 7.31 (m, 3H), 7.16 (d, J = 8.3 Hz, 1H), 6.90 (d, J = 9.10 Hz, 2H), 3.57 (s, 3H), 3.03 (s, 6H). LCMS found, 319 $[M + H]^+$.

2-(4-((3′-Amino-[3,6′-biquinolin]-4′-yl)amino)phenyl)-2-methylpropanenitrile (20). Prepared using General Procedure E, reacting compound **13** and 3-quinoline boronic acid. Purification was carried out by flash column chromatography over silica gel (eluent: CH_2Cl_2/MeOH 100:0 to 95:5) to give **20** as a pale yellow solid (yield: 2%). ^{1}H NMR (400 MHz, DMSO-d_6) δ ppm: 9.23 (d, J = 2.3 Hz, 1H), 8.63 (s, 2H), 8.16 (m, 1H), 8.09 (s, 1H), 8.02 (m, 3H), 7.87 (dd, J = 8.8, 2.0 Hz, 1H), 7.76 (m, 1H), 7.64 (m, 1H), 7.28 (d, 8.8 Hz, 2H), 6.63 (d, J = 8.8 Hz, 2H), 5.30 (brs, 2H), 1.60 (s, 6H). LCMS found, 430 $[M + H]^+$.

4-(3-Methyl-2-oxo-1-(*p*-tolyl)-2,3-dihydro-1*H*-imidazo[4,5-*c*]-quinolin-8-yl)benzoic Acid (21). Prepared using General Procedure E, reacting intermediate **15e** with 4-carboxyphenyl boronic acid. Purification was carried out by flash column chromatography over silica gel (eluent: CH_2Cl_2/MeOH 100:0 to 90:10) to give **21** as a yellow solid (yield: 27%). ^{1}H NMR (400 MHz, DMSO-d_6) δ ppm: 9.00 (s, 1H), 8.10 (d, J = 9.1 Hz, 1H), 7.93 (m, 3H), 7.54 (m, 4H), 7.39 (d, J = 8.3 Hz, 2H), 7.21 (d, J = 1.3 Hz, 1H), 3.61 (s, 3H), 3.31 (s, 3H). LCMS found, 410 $[M + H]^+$.

3,8-Dimethyl-1-phenyl-1*H*-imidazo[4,5-*c*]quinolin-2(3*H*)-one (22). Prepared from intermediate **15c** using General Procedure G.

dx.doi.org/10.1021/jm500361r | *J. Med. Chem.* 2014, 57, 4834−4848

Compound **22** was obtained as a white solid (yield: 17%). ^{1}H NMR (400 MHz, DMSO-d_6) δ ppm: 8.92 (s, 1H), 7.92 (d, J = 8.8 Hz 1H), 7.67 (m, 3H), 7.59 (m, 2H), 7.38 (dd, J = 8.8, 1.8 Hz, 1H), 6.70 (s, 1H), 3.58 (s, 3H), 2.16 (s, 3H). LCMS found, 290 $[M + H]^+$.

3-Methyl-1-phenyl-1*H*-imidazo[4,5-*c*]quinolin-2(3*H*)-one (23). Prepared using General Procedure E, reacting intermediate **15c** with trimethylboroxin. Purification was carried out by flash column chromatography over silica gel (eluent: CH_2Cl_2/MeOH 100:0 to 95:5) to give **23** as an off-white solid (yield: 33%, purity: 94%). ^{1}H NMR (400 MHz, DMSO-d_6) δ ppm: 9.01 (s, 1H), 8.03 (d, J = 7.8 Hz, 1H), 7.6 (m, 6H), 7.29 (m, 1H), 6.99 (d, J = 8.6 Hz, 1H), 3.59 (s, 3H). LCMS found, 276 $[M + H]^+$.

Cellular Activity Assays. *Trypanosome Cell Culture and Cell Growth Assays.* Bloodstream *Trypanosoma brucei brucei* Lister 427 was the selected strain to perform the HTS experiments and the profiling assay. The cell strain was cultured in Hirumi's modified Iscove's medium (HMI-9)[29] supplemented with 10% heat-inactivated FBS at 37 °C and 5% CO_2 in T-25 vented flasks (Corning). We evaluated the anti-trypanosomal activity of the newly prepared compounds in *Trypanosoma brucei brucei* culture according to resazurin viability test.

Dose–Response Assay. For dose–response experiments, serial dilutions of compounds were plotted against compound concentration. Dose–response starting at 10 mM, unless indicated, with 3-fold dilutions for 11 points were made in masterplates. Two hundred nanoliters per well from those masterplates was stamped in final assay plates. Controls of 0% response (control 1, 0.2 μL of 100% DMSO) and 100% response (control 2, 0.2 μL of 1 mM Pentamidine) were included in each assay plate in columns 6 and 18, respectively. Plates containing 0.2 μL of 100% DMSO were included in the assay to assess quality through the entire process. To detect growth inhibition, parasites in log phase growth were diluted to a working concentration of 2500 cells/mL in prewarmed HMI-9 medium and gently stirred until dispensation. Fifty microliters of culture was dispensed in compound-stamped black, clear-bottom, 384-well Greiner microplates using a Multidrop Combi Reagent Dispenser (Thermo Scientific) to give a final solvent concentration of 0.4% DMSO. Plates were covered with a lid, and cells were incubated for 70 h at 37 °C and 5% CO_2. After this period, 10 μL of 200 μM resazurin solution in prewarmed HMI-9 was added to each well, and plates were allowed to incubate 2 h more prior to fluorescence reading in a Wallac EnVision multilabel plate reader (PerkinElmer). Raw fluorescent data from the Envision plate reader were uploaded into GSK HTS database (ActivityBase). Activity of each well was normalized as a percentage of inhibition on a per-plate basis using the following equation

$$\%\ \text{inhibition} = 100 - \frac{100 \times \text{test well} - \text{median CTRL1}}{\text{median CTRL1} - \text{median CTRL2}}$$

where control 1 represents wells from the same plate containing 0.4% DMSO (0% inhibition, 100% grown control, n = 16) and control 2 represents wells from the same plate treated with pentamidine (100% inhibition, 0% grown, n = 16). A Z' value greater than 0.4 was required for plate validation during the quality control process.

A four-parameter equation describing a sigmoidal dose–response curve was then fitted with an adjustable baseline using ActivityBase XE Runner software. Fitting of dose–response curves and EC_{50} determination were normalized as percentage of inhibition based on controls. The curve-fit model was based on a four-parameter logistic equation

$$Y = \text{min} + \frac{\text{max} - \text{min}}{1 + \left(\frac{10^{\log_{10}\text{cmpd conc(M)}}}{10^{\log_{10}\text{EC50}}}\right)^{\text{slope factor}}}$$

HepG2 Cell Culture and Growth Assays. The HepG2 cell line (human liver hepatocellular carcinoma cell line, ATCC) was cultured in Eagle's MEM supplemented with L-glutamine, Earle's salts, 10% heat-inactivated FBS, and 1% non-essential amino acids (NEAA) at 37 °C and 5% CO_2 in T-175 vented flasks (Corning). The human biological samples were sourced ethically, and their research use was in accord with the terms of informed consent.

Cytotoxicity Assay. This assay was used as a selectivity assay, and compounds were tested at dose–response concentrations against HepG2 in order to identify the level of cytotoxicity. Dose– response starting at 10 mM, unless indicated, with 3-fold dilutions for 11 points was made in master plates (1536). Fifty nanoliters per well was stamped in final assay plates.

Log-phase HepG2 cells were removed from a T-175 TC flask using cell dispersion medium and dispersed by repeated pipetting. Cell density was adjusted to 60 000 cells/mL as the working concentration in prewarmed Eagle's MEM. The seeding density was checked to ensure that new monolayers were not more than ∼50% confluent at the time of seeding (typically 3000 cells per well), before completing preparation of the plates. Five microliters of culture was dispensed in compound-stamped TC treated, Greiner white 1536-well plates using a Multidrop Combi Reagent Dispenser (Thermo Scientific) to a final concentration of 1% DMSO. Cells were incubated for 48 h at 37 °C and 5% CO_2. Viability was determined by CellTiter-Glo kit (Promega) according to the manufacturer's instructions. Briefly, reconstituted CellTiter Buffer was equilibrated to room temperature prior use, and 5 μL per well was dispensed with a Multidrop Combi Reagent Dispenser. Contents were mixed on a plate orbital shaker and incubated for 10 min at room temperature to allow the signal to stabilize before luminescence reading on ViewLux Plate Reader (PerkinElmer).

Raw luminescence data from the ViewLux reader were uploaded into GSK HTS database (ActivityBase). Activity of each well was normalized as a percentage of inhibition on a per-plate basis using the following equation

$$\%\ \text{inhibition} = 100 - 100 \times \frac{\text{test well} - \text{median CTRL1}}{\text{median CTRL1} - \text{median CTRL2}}$$

where control 1 represents wells from the same plate containing 1% DMSO (0% inhibition, 100% grown control, n = 128) and control 2 represents wells from the same plate treated with digitoxin (100% inhibition, 0% grown, n = 128). A Z' value greater than 0.4 was required for plate validation during the quality control process.

As previously described for the primary assay, a four-parameter equation describing a sigmoidal dose–response curve was then fitted with an adjustable baseline using ActvityBase XE Runner software.

Phospholipidomics Analyses. *Lipid Extraction.* Total lipids from mid log phase cells were extracted by the method of Bligh and Dyer.[30] Briefly, mid log phase cells were collected by centrifugation (800*g*, 10 min), washed with PBS, resuspended in 100 μL of TDB-glucose, transferred to a glass tube containing 375 μL of 1:2 (v/v) $CHCl_3$/MeOH, and vortexed. The sample was agitated vigorously for a further 10–15 min. The sample was made biphasic by the addition of 125 μL of $CHCl_3$ and vortexed, and then 125 μL of H_2O was added. The sample was vortexed again and centrifuged at 3000*g* at rt for 10 min. The lower (organic) phase was transferred into a new glass vial, and the aqueous phase was re-extracted with the fresh lower phase. The resultant lower phase lipid extract was dried under a stream of nitrogen and stored at 4 °C.

Electrospray Mass Spectrometry Analysis. Lipid extracts were dissolved in 15 μL of $CHCl_3$/MeOH (1:2) and 15 μL of acetonitrile/isopropanol/water (6:7:2) and analyzed with a triple quadrupole mass spectrometer (Absceix 4000 QTrap) equipped with a nanoelectrospray source. Samples were delivered into the spectrometer using either thin-walled nanoflow capillary tips or a Nanomate interface in direct infusion mode (∼125 nL/min). The lipid extracts were analyzed in both positive and negative ion modes using a capillary voltage of 1.25 kV. MS/MS scanning (daughter, precursor, and neutral loss scans) were performed using nitrogen as the collision gas, with collision energies between 35 and 90 V. Each spectrum encompasses at least 50 repetitive scans. Tandem mass spectra (MS/MS) were obtained with collision energies as follows: 35–45 V, PC/SM in positive ion mode, parent-ion scanning of m/z 184; 35–55 V, PI in negative ion mode, parent-ion scanning of m/z 241; 35–65 V, PE in negative ion mode, parent-ion scanning of m/z 196; 20–35 V, PS in negative ion mode, neutral loss scanning of m/z 87; and 40–90 V, for all glycerophospholipids (including PA, PG, and cardiolipin) detected

dx.doi.org/10.1021/jm500361r | J. Med. Chem. 2014, 57, 4834–4848

by precursor scanning for m/z 153 in negative ion mode. MS/MS daughter ion scanning was performed with collision energies between 35 and 90 V.

Assignment of phospholipid species was based upon a combination of survey, daughter, precursor, and neutral loss scans as well previous assignments.[31] The identity of phospholipid peaks was verified using the LIPID MAPS: Nature Lipidomics Gateway (www.lipidmaps.org).

Cellular Phenotype Analyses. *Transferrin Uptake.* Two million trypanosomes were harvested and washed with TDB-glucose plus 1% BSA, resuspended in 250 μL in the same buffer, and incubated for 10 min at 37 °C prior to the addition of 5 μg of AlexaFluor 488-conjugated human holo-Tf (Invitrogen). Incubations were carried out for 0 (no Tf) or 3 min at 37 °C, after which cells were immediately fixed in 4 °C in 1% PFA diluted in cold PBS for at least 1 h. Parasites were finally washed twice with PBS and analyzed with a Becton Dickinson FACSCalibur flow cytometer (BD Biosciences) using BD CellQuest Pro version 4.0.2 software.

FACS Analysis. For cell cycle analysis, samples (1.5×10^6 cells) were collected, centrifuged (1400*g* at 4 °C for 5 min), and washed in trypanosome dilution buffer (TDB). The cell pellets were gently suspended in 50 μL of TDB and permeabilized by adding 1 μL of saponin (25 mg/mL) for 3 min. It was then mixed with another 450 μL of TDB. RNase and propidium iodide (PI) were added to the suspension at final concentrations of 10 and 20 μg/mL, respectively, and the samples were incubated at room temperature for 30 min and then stored at 4 °C. The DNA content of PI-stained cells and the percentage of cells in each phase of the cell cycle (10 000 cells per sample) were analyzed with a Becton Dickinson FACSCalibur flow cytometer (BD Biosciences) using BD CellQuest Pro version 4.0.2 software.

■ ASSOCIATED CONTENT

Ⓢ Supporting Information

Additional mass spectrometry data; data tables from this article annotated with NEU registry numbers; and biochemical and physicochemical assay details. This material is available free of charge via the Internet at http://pubs.acs.org. All of the data included in this work has also been made available as a publically available data set on www.collaborativedrug.com.

■ AUTHOR INFORMATION

Corresponding Authors

*(M.N.) Phone: +34 958 181651; E-mail: miguel.navarro@ipb.csic.es.

*(M.P.P.) Phone: 617-373-2703; E-mail: m.pollastri@neu.edu.

Notes

The authors declare no competing financial interest.

■ ACKNOWLEDGMENTS

This work was supported in part by the Tres Cantos Open Lab Foundation (M.P.P., M.N., R.D., S.L.-A., and J.D.S.), NIH 7R01AI082577 (M.P.P.), and Wellcome Trust grant 093228 (T.K.S.). M.S., D.R., and M.N. are supported by grants from the Spanish MICINN (SAF2012-40029), Junta de Andalucia (CTS-5841), and RICET (RD12/0018).

■ ABBREVIATIONS USED

HAT, human African trypanosomiasis; SAR, structure−activity relationships; PI3K, phosphoinositol-3-kinase; mTOR, mammalian target of rapamycin; CNS, central nervous system; LE, ligand efficiency; PIP, phosphatidylinositol phosphate; TDB, trypanosome dilution buffer; PBS, phosphate buffered saline; PFA, paraformaldehyde; GSK, GlaxoSmithKline; PIKK, Phosphatidyl inositol 3′-kinase-related kinase

■ REFERENCES

(1) World Health Organization. *Sustaining the drive to overcome the global impact of neglected tropical diseases.* http://apps.who.int/iris/bitstream/10665/77950/1/9789241564540_eng.pdf (accessed April 22, 2014).

(2) Jacobs, R. T.; Nare, B.; Phillips, M. A. State of the art in African trypanosome drug discovery. *Curr. Top. Med. Chem.* **2011**, *11*, 1255−1274.

(3) Target Product Profile for Human African Trypanosomiasis. http://www.dndi.org/diseases-projects/diseases/hat/target-product-profile.html (accessed March 23, 2013).

(4) Pollastri, M. P.; Campbell, R. K. Target repurposing for neglected diseases. *Future Med. Chem.* **2011**, *3*, 1307−1315.

(5) Page, T. H.; Smolinska, M.; Gillespie, J.; Urbaniak, A. M.; Foxwell, B. M. Tyrosine kinases and inflammatory signalling. *Curr. Mol. Med.* **2009**, *9*, 69−85.

(6) Ito, K.; Caramori, G.; Adcock, I. M. Therapeutic potential of phosphatidylinositol 3-kinase inhibitors in inflammatory respiratory disease. *J. Pharmacol. Exp. Ther.* **2007**, *321*, 1−8.

(7) Chahrour, O.; Cairns, D.; Omran, Z. Small molecule kinase inhibitors as anti-cancer therapeutics. *Mini-Rev. Med. Chem.* **2012**, *12*, 399−411.

(8) Hopkins, A. L.; Groom, C. R. The druggable genome. *Nat. Rev. Drug. Discovery* **2002**, *1*, 727−730.

(9) Johannessen, L. E.; Ringerike, T.; Molnes, J.; Madshus, I. H. Epidermal growth factor receptor efficiently activates mitogen-activated protein kinase in HeLa cells and Hep2 cells conditionally defective in clathrin-dependent endocytosis. *Exp. Cell Res.* **2000**, *260*, 136−145.

(10) Naula, C.; Parsons, M.; Mottram, J. C. Protein kinases as drug targets in trypanosomes and *Leishmania*. *Biochim. Biophys. Acta* **2005**, *1754*, 151−159.

(11) Oduor, R. O.; Ojo, K. K.; Williams, G. P.; Bertelli, F.; Mills, J.; Maes, L.; Pryde, D. C.; Parkinson, T.; Van Voorhis, W. C.; Holler, T. P. *Trypanosoma brucei* glycogen synthase kinase-3, a target for anti-trypanosomal drug development: A public−private partnership to identify novel leads. *PLoS Neglected Trop. Dis.* **2011**, *5*, e1017.

(12) Diaz-Gonzalez, R.; Kuhlmann, F. M.; Galan-Rodriguez, C.; Madeira da Silva, L.; Saldivia, M.; Karver, C. E.; Rodriguez, A.; Beverley, S. M.; Navarro, M.; Pollastri, M. P. The susceptibility of trypanosomatid pathogens to PI3/mTOR kinase inhibitors affords a new opportunity for drug repurposing. *PLoS Neglected Trop. Dis.* **2011**, *5*, e1297.

(13) Ochiana, S. O.; Pandarinath, V.; Wang, Z.; Kapoor, R.; Ondrechen, M. J.; Ruben, L.; Pollastri, M. P. The human Aurora kinase inhibitor danusertib is a lead compound for anti-trypanosomal drug discovery via target repurposing. *Eur. J. Med. Chem.* **2013**, *62*, 777−784.

(14) Patel, G.; Karver, C. E.; Behera, R.; Guyett, P. J.; Sullenberger, C.; Edwards, P.; Roncal, N. E.; Mensa-Wilmot, K.; Pollastri, M. P. Kinase scaffold repurposing for neglected disease drug discovery: Discovery of an efficacious, lapatanib-derived lead compound for trypanosomiasis. *J. Med. Chem.* **2013**, *56*, 3820−3832.

(15) Katiyar, S.; Kufareva, I.; Behera, R.; Thomas, S. M.; Ogata, Y.; Pollastri, M.; Abagyan, R.; Mensa-Wilmot, K. Lapatinib-binding protein kinases in the African trypanosome: identification of cellular targets for kinase-directed chemical scaffolds. *PLoS One* **2013**, *8*, e56150.

(16) Maira, S.-M.; Stauffer, F.; Brueggen, J.; Furet, P.; Schnell, C.; Fritsch, C.; Brachmann, S.; Chène, P.; De Pover, A.; Schoemaker, K.; Fabbro, D.; Gabriel, D.; Simonen, M.; Murphy, L.; Finan, P.; Sellers, W.; García-Echeverría, C. Identification and characterization of NVP-BEZ235, a new orally available dual phosphatidylinositol 3-kinase/mammalian target of rapamycin inhibitor with potent in vivo antitumor activity. *Mol. Cancer Ther.* **2008**, *7*, 1851−1863.

(17) Cheng, H.; Li, C.; Bailey, S.; Baxi, S. M.; Goulet, L.; Guo, L.; Hoffman, J.; Jiang, Y.; Johnson, T. O.; Johnson, T. W.; Knighton, D. R.; Li, J.; Liu, K. K. C.; Liu, Z.; Marx, M. A.; Walls, M.; Wells, P. A.; Yin, M.-J.; Zhu, J.; Zientek, M. Discovery of the highly potent PI3K/

mTOR dual inhibitor PF-04979064 through structure-based drug design. *ACS Med. Chem. Lett.* **2012**, *4*, 91−97.
(18) Wager, T. T.; Hou, X.; Verhoest, P. R.; Villalobos, A. Moving beyond rules: The development of a central nervous system multiparameter optimization (CNS MPO) approach to enable alignment of druglike properties. *ACS Chem. Neurosci.* **2010**, *1*, 435−449.
(19) Engelhardt, H.; Kofink, C.; McConnell, D. Preparation of heterocyclic carboxylic acid amides as PDK1 inhibitors. Patent WO2011131741A1, 2011.
(20) Stauffer, F.; Maira, S.-M.; Furet, P.; García-Echeverría, C. Imidazo[4,5-c]quinolines as inhibitors of the PI3K/PKB-pathway. *Bioorg. Med. Chem. Lett.* **2008**, *18*, 1027−1030.
(21) Valko, K.; Bevan, C.; Reynolds, D. Chromatographic hydrophobicity index by fast-gradient RP-HPLC: A high-throughput alternative to log P/log D. *Anal. Chem.* **1997**, *69*, 2022−2029.
(22) Bhattachar, S. N.; Wesley, J. A.; Seadeek, C. Evaluation of the chemiluminescent nitrogen detector for solubility determinations to support drug discovery. *J. Pharm. Biomed. Anal.* **2006**, *41*, 152−157.
(23) Wager, T. T.; Chandrasekaran, R. Y.; Hou, X.; Troutman, M. D.; Verhoest, P. R.; Villalobos, A.; Will, Y. Defining desirable central nervous system drug space through the alignment of molecular properties, in vitro ADME, and safety attributes. *ACS Chem. Neurosci.* **2010**, *1*, 420−434.
(24) Heffron, T. P.; Salphati, L.; Alicke, B.; Cheong, J.; Dotson, J.; Edgar, K.; Goldsmith, R.; Gould, S. E.; Lee, L. B.; Lesnick, J. D.; Lewis, C.; Ndubaku, C.; Nonomiya, J.; Olivero, A. G.; Pang, J.; Plise, E. G.; Sideris, S.; Trapp, S.; Wallin, J.; Wang, L.; Zhang, X. The design and identification of brain penetrant inhibitors of phosphoinositide 3-kinase α. *J. Med. Chem.* **2012**, *55*, 8007−8020.
(25) Hall, B. S.; Gabernet-Castello, C.; Voak, A.; Goulding, D.; Natesan, S. K.; Field, M. C. TbVps34, the trypanosome orthologue of Vps34, is required for Golgi complex segregation. *J. Biol. Chem.* **2006**, *281*, 27600−27612.
(26) Barquilla, A.; Crespo, J. L.; Navarro, M. Rapamycin inhibits trypanosome cell growth by preventing TOR complex 2 formation. *Proc. Natl. Acad. Sci. U.S.A.* **2008**, *105*, 14579−14584.
(27) de Jesus, T. C.; Tonelli, R. R.; Nardelli, S. C.; da Silva Augusto, L.; Motta, M. C.; Girard-Dias, W.; Miranda, K.; Ulrich, P.; Jimenez, V.; Barquilla, A.; Navarro, M.; Docampo, R.; Schenkman, S. Target of rapamycin (TOR)-like 1 kinase is involved in the control of polyphosphate levels and acidocalcisome maintenance in *Trypanosoma brucei*. *J. Biol. Chem.* **2010**, *285*, 24131−24140.
(28) Meng, F.; Zhu, X.; Li, Y.; Xie, J.; Wang, B.; Yao, J.; Wan, Y. Efficient copper-catalyzed direct amination of aryl halides using aqueous ammonia in water. *Eur. J. Org. Chem.* **2010**, *2010*, 6149−6152.
(29) Hirumi, H.; Hirumi, K. Continuous cultivation of *Trypanosoma brucei* blood stream forms in a medium containing a low concentration of serum protein without feeder cell layers. *J. Parasitol.* **1989**, *75*, 985−989.
(30) Bligh, E. G.; Dyer, W. J. A rapid method of total lipid extraction and purification. *Can. J. Biochem. Physiol.* **1959**, *37*, 911−917.
(31) Richmond, G. S.; Gibellini, F.; Young, S. A.; Major, L.; Denton, H.; Lilley, A.; Smith, T. K. Lipidomic analysis of bloodstream and procyclic form *Trypanosoma brucei*. *Parasitology* **2010**, *137*, 1357−1392.